Genetic loci of the *R. anatipestifer* serotype discovered by Pan-GWAS and its application for the development of a multiplex PCR serotyping method

Zhishuang Yang[1,3], Xueqin Yang[1,3], Mingshu Wang[1,2,3], Renyong Jia[1,2,3], Shun Chen[1,2,3], Mafeng Liu[1,2,3], Xinxin Zhao[1,2,3], Qiao Yang[1,2,3], Ying Wu[1,2,3], Shaqiu Zhang[1,2,3], Juan Huang[1,2,3], Xumin Ou[1,2,3], Sai Mao[1,2,3], Qun Gao[1,2,3], Di Sun[1,2,3], Bin Tian[1,2,3], Dekang Zhu[1,3*], Anchun Cheng[1,2,3*]

[1]Research Center of Avian Diseases, College of Veterinary Medicine, Sichuan Agricultural University, Chengdu, Sichuan, China.

[2]Institute of Preventive Veterinary Medicine, Sichuan Agricultural University, Chengdu, Sichuan, China.

[3]Key Laboratory of Animal Disease and Human Health of Sichuan Province, Chengdu, Sichuan, China.

* Corresponding author:

Dekang Zhu, Email: zdk24@sicau.edu.cn; Anchun Cheng, Email: chenganchun@vip.163.com

Email address:

Zhishuang Yang, yangzs_chi@yeah.net; Xueqin Yang, yangxueqin@live.cn; Mingshu Wang, mshwang@163.com; Renyong Jia, jiary@sicau.edu.cn; Shun Chen, shunchen@sicau.edu.cn; Mafeng Liu, liumafengra@163.com; Xinxin Zhao, xxinzhao@sicau.edu.cn; Qiao Yang, yangqiao721521@sina.com; Ying Wu, yingzi_no1@126.com; Shaqiu Zhang, shaqiu86@hotmail.com; Xumin Ou, x.ou@sicau.edu.cn; Sai Mao, sarrawin@163.com; Qun Gao, 592681288@qq.com; Di Sun, sundi0921@163.com; Dekang Zhu, zdk24@sicau.edu.cn; Anchun Cheng,

chenganchun@vip.163.com

Highlights

1. *R. anatipestifer* serotype-specific locus was identified by Pan-GWAS for the first time.
2. Molecular serotyping multiplex PCR was developed based on O-antigen biosynthesis gene clusters

Abstract

The disease caused by *Riemerella anatipestifer* (*R. anatipestifer*) causes large economic losses to the global duck industry every year. Serotype-related genomic variation (such as in O-antigen and capsular polysaccharide gene clusters) has been widely used for the serotyping in many gram-negative bacteria. To date, there have been few studies focused on genetic basis of serotypes in *R. anatipestifer*. Here, we used pan-genome-wide association studies (Pan-GWAS) to identify the serotype-specific genetic loci of 38 *R. anatipestifers* strain. Analyses of the loci of 11 serotypes showed that the loci could be well mapped with the serotypes of the corresponding strains. We constructed the knockout strain for the *wzy* gene at the locus, and the results showed that the mutant lost the agglutination characteristics to positive antisera. Based on the of Pan-GWAS results, we developed a multiple PCR method to identify serotypes 1, 2, and 11 of *R. anatipestifer*. Our study provides a precedent for systematically analysing the genetic basis of the *R anatipestifer* serotypes and establishing a complete serotyping system in the future.

Key words: *Riemerella anatipestifer*; Pan-genome-wide association studies; O-antigen gene cluster; Serotyping; multiplex PCR.

Introduction

R. anatipestifer attacks domestic ducks, geese, and turkeys and causes an acute or chronic septicaemia characterized by fibrinous pericarditis, perihepatitis, airsacculitis, caseous salpingitis, and meningitis(Boulianne et al.). Since 1982, when Bisgaard(Bisgaard, 1982) established the *R. anatipestifer* serotyping scheme (labelled with Arabic numerals), at least 21 serotypes have been reported around the world(Pathanasophon et al., 2002). There is no effective cross-protection among different serotypes(Liao et al., 2015). Unfortunately, no molecular serotyping method for *R. anatipestifer* has been proposed.

In most gram-negative bacteria, the surface O-antigen structures exhibit intraspecies diversity, which is usually associated with serotypes(Bian et al., 2020; Carter, 1955; Kenyon et al., 2017; Liu et al., 2014; Townsend et al., 2001). The diversity of O-antigens is attributed to genetic variation in O-antigen gene clusters (O-AGCs), which provides a target for molecular serotyping(Fang et al., 2016; Franklin et al., 2011; Liu et al., 2020). Notably, due to the high correlation between the genetic signature of O-AGCs and the serotype phenotype, O-antigen synthesis-related genes (e.g. *wzy*, *wzx* etc.) have been widely used as targets for molecular serotyping of many gram-negative bacteria(Fang et al., 2016; Iguchi et al., 2020; Townsend et al., 2001; Wang et al., 2017a; Xi et al., 2019; Zeng et al., 2019).

Genome-wide association studies (GWAS) have become a powerful tool in bacteria to uncover the genetic basis of some important phenotypes, such as virulence and antibiotic resistance(Farhat et al., 2019; Ma et al., 2020; Young et al., 2019; Yuan et al., 2019; Zankari et al., 2013). In the current study, we used GWAS to identify the genetic loci associated with serotypes and demonstrated that these loci are located within the same genomic region of *R. anatipestifer*. Furthermore, we analysed the genetic diversity of the genetic locus in *R. anatipestifer* (11 serotypes). Based on the genetic variation, we present a multiplex PCR (mPCR) method for the identification of the major serotypes of *R. anatipestifer*, which provides a potential method for epidemiological surveillance of this pathogen.

Materials and methods

Bacterial strain

The *R. anatipestifer* strains and the published genome data employed in this study are listed in Supplementary Table 1.

Agglutination test using the antisera

The serotypes of *R. anatipestifer* involved in this study were determined by slide agglutination according to Brogden et al.(Bisgaard, 1982). Standard typing antisera were purchased from RIPAC-LABOR GmbH (Potsdam, Germany). The *R. anatipestifer* strains were grown on tryptic soy agar (TSA), enriched with 5% sheep blood, at 37°C for 24 h under microaerophilic conditions.

Genome wide association study of serotypes

To explore the association between *R. anatipestifer* serotypes and genetic characteristics, a pan-genome-wide association study (Pan-GWAS) was performed. Specifically, the *R. anatipestifer* genome was annotated using Prokka v1.12 (Seemann, 2014), and the pan-genome containing 38 strains of *R. anatipestifer* was reconstructed with Roary (Version 3.12.0, with identity threshold of protein = 90)(Page et al., 2015). Furthermore, Scoary(v1.6.16)(Brynildsrud et al., 2016) was used to perform the Pan-GWAS with the *gene_presence_absence* file generated by Roary (only serotypes containing more than 4 strains were considered). Scoary's P-value and Q-value (P-adjust, adjust algorithm: Benjamini-Hochberg method) cut-offs were set to < 0.05, the sensitivity cut-off was set to 70% and specificity to 85%. Next, we mapped the genes that were significantly associated with the serotype to the corresponding genome to obtain the distribution characteristics. Contig comparisons were generated with Easyfig (v2.2)(Sullivan et al., 2011).

Functional speculation of the gene cluster

To explore the function of serotype-related genetic loci, genome-wide biosynthetic gene clusters (BGCs) of *R. anatipestifer* was predicted with antiSMASH (version 4.2.0, parameter setting: --clusterblast --subclusterblast --knownclusterblast --smcogs --inclusive --borderpredict) (Blin et al., 2017). AntiSMASH also searches for the most similar gene clusters against the Minimum Information about a Biosynthetic Gene Cluster (MIBiG) database(Medema et al., 2015).

BGCs analysis was performed again by DeepBGC (Hannigan et al., 2019), which uses deep learning strategies to mine biosynthetic gene clusters in the microbial genome. The results of the above two methods will be considered comprehensive.

Gene boundary determination of *R. anatipestifer* O-AGCs

Based on the results of biosynthetic gene cluster mining, we further determined the boundaries of the *R. anatipestifer* O-antigen gene cluster.

More specifically, we retrieved 509 known O-antigen gene clusters from the NCBI Nucleotide database (https://www.ncbi.nlm.nih.gov/nuccore), which included *Enterobacter*, *Salmonella*, *Yersinia*, etc. (Supplementary Table 2). We downloaded the protein sequence of these gene clusters, used CD-HIT (version 4.8.1, parameter setting: -c 1 -aS 0.95)(Li and Godzik, 2006) to remove redundancies and constructed the O-antigen synthesis gene database. Tblastn was used to map these proteins to the *R. anatipestifer* genome, and the resulting filtering thresholds were as follows: coverage ≥50% (-qcov_hsp_perc 50), e-value≤ 1e-5 (-evalue 1e-5). Subsequently, the densely mapped regions in the genome are considered as candidates for the O-antigen gene cluster. Finally, combined with the prediction results of BGCs, the boundary of the O-antigen gene cluster was determined by manual inspection.

Annotation of the O-AGCs

Protein-encoding genes were predicted using Prokka v1.12 (Seemann, 2014) with default parameters. To assign functions to the predicted genes, the Conserved Domains Database (CDD)(Marchler-Bauer et al., 2014) was used to search for

conserved domains with an E-value threshold of 0.01. Meanwhile characteristic gene annotation of genes was performed using Blastp (v2.6+) against Non-Redundant (NR, https://ftp.ncbi.nlm.nih.gov/blast/db/FASTA/nr.gz). The E-value and query coverage were set at 1e-5 and 50% respectively.

To identify the O-antigen translocase (Wzx) and O-antigen polymerase (Wzy), TMHMM2.0(Krogh et al., 2001) was used to predict the transmembrane regions of proteins.

Inter- and intra-serotypes comparison of LPS GCs

wzx, *wzy* and O-antigen gene cluster nucleotide sequence alignment was performed using MAFFT (Katoh et al., 2002) in automatic mode, and then Mega 7(Kumar et al., 2016) with default parameters and 1000 bootstrap replicates were used to reconstruct the NJ (neighbor joining)(Saitou and Nei, 1987) phylogenetic tree.

Blast (v2.6+) and Easyfig (v2.2)(Sullivan et al., 2011) were used for inter- and intra-serotype O-antigen gene cluster comparisons. DNAMAN (version 9, Lynnon Corp., Quebec, Canada) was used to calculate the percentage homology of protein and DNA sequences.

Conservation analysis of genetic locus in *Flavobacteriaceae*

To show the conservation of our gene cluster in *Flavobacteriaceae*, the multi-gene search method was implemented. Specifically, Multigeneblast(Medema et al., 2013) was used to find homologues of *R. anatipestifer* O-AGCs from the representative genomes of all species of *Flavobacteriaceae* species. In addition, we

used Easyfig (v2.2) to analyse the conservation of the best homologues at the corresponding genus level.

Development of a multiplex serotyping PCR

Based on the sequence variation in the serotype-specific genes of the O-antigen gene cluster, we designed a primer set with Primer-blast (https://www.ncbi.nlm.nih.gov/tools/primer-blast/index.cgi) and MFEprimer3(Qu and Zhang, 2015) , that contains 4 primer pairs to specifically detect each of the 3 *R. anatipestifer* serotypes (Table 2). Three primer pairs Primer_1, Primer_2, and Primer_11 were designed to detect serotypes 1, 2, and 11 respectively. The Primer_RA primer pair serves as an internal control, it can detect all *R. anatipestifer*. Each reaction mixture (25 μl) contained 1 μl template DNA, 12.5 μl Premix Taq (TaKaRa Taq^{TM} Version 2.0 plus dye), Primer_1 (2×0.1 μl), Primer_2 (2×0.2 μl), Primer_11 (2×1 μl) and Primer_RA (2×0.5 μl).

PCR was conducted with initial denaturation for 5 min at 95°C, followed by 35 cycles of 30 s at 95°C, 30 s at 57.9°C and 1 min at 72°C. PCR products were analysed by agarose gel electrophoresis using 1.5% agarose

To evaluate the performance of mPCR, we tested 181 serotype known isolates (n=45, serotype 1; n=79, serotype 2; n=49, serotype 11; n=8, other serotypes) by single-blind method. Cohen's kappa statistics were performed by R software (version 4.0.3, https://www.r-project.org/) with the package fmsb (version 0.7.0, http://minato.sip21c.org/msb/).

Construction of *R. anatipestifer wzy* mutant strain CH-2Δ*wzy*

The *wzy* gene (G148_RS04365) was deleted by allelic exchange using the recombinant suicide vector pYA4278 (Kong et al.(Leclercq and Courvalin, 1991); donated by Professor Kong). Briefly, upstream (L) and downstream (R) fragments of the *R. anatipestifer* CH-2 *wzy* gene were amplified by PCR from the genome using *wzy*-Left F and *wzy*-Left R, and *wzy*-Right F and *wzy*-Right R primers, respectively. A 1145-bp $Spec^R$ cassette was PCR-amplified from the pYES1 new plasmid using the Spc F and Spc R primers. The three fragments were then spliced together in vitro by overlap extension using the *wzy*-Left F and *wzy*-Right R primers, producing the LSR fragment. Adenosine nucleotides were added to both ends of the PCR product, which was then ligated to the AhdI-digested T-cloning suicide vector pYA4278 to generate pYA4278-LSR, which carries a deletion of the entire *wzy* gene. Subsequently, pYA4278-LSR was successively transformed into *E. coli X7232* and *E. coli* X7213λpir(Edwards et al., 1998). *E. coli* X7213λpir (Donor) and *R. anatipestifer* CH-2 (Recipient) were mixed in a 10-mM $MgSO_4$ solution and incubated on TSB agar with diaminopimelic acid at 37°C for 24 h. $Spec^R$ transconjugants were further selected in media containing spectinomycin (40 μg/ml). The detailed steps of this study refer to the methods of Luo et al.(Luo et al., 2015). To confirm the *R. anatipestifer* mutant CH-2Δ*wzy*, we performed PCR targeting the transconjugants (see Figure 12 for details). The primers are listed in Table 2.

Results

The serotypes of *R. anatipestifer*

In this study, *R. anatipestifer* involved a total of 11 serotypes, including Serotype 1 (n=7), Serotype 2 (n=12), Serotype 3 (n=1), Serotype 4 (n=1), Serotype 5 (n=1), Serotype 6 (n=3), Serotype 7 (n=3), Serotype 8 (n=1), Serotype 10 (n=5), Serotype 11 (n=4), and Serotype 12 (n=1), which were determined by slide agglutination or from references. All strains and their serotypes are shown in Supplementary Table 1.

Serotype phenotype of *R. anatipestifer* associated with the gene cluster

To screen for loci associated with serotypes, a GWAS was performed with Scoary on the serotypes containing more than 4 strains (serotypes 1, 2, 10, 11). Under the filtering conditions mentioned in the methods, we obtained a total of 31 target genes. The numbers of genes associated with serotype 1, serotype 2, serotype 10 and serotype 11 were 8, 9, 5 and 8, respectively. The minimum specificity and minimum sensitivity of genes significantly related to the serotype were 85.19% (Serotype 2) and 71.43% (Serotype 1), respectively (Supplementary Table 3). Next, we mapped these genes to the corresponding genome and found that these genes were close to each other and formed a gene cluster. Interestingly, according to the BGCs results predicted by antiSMASH, the gene clusters mentioned above were labelled as lipopolysaccharide biosynthetic gene clusters (Table 1). Thirteen percent of the genes in the gene clusters show similarity with the *Legionella pneumophila* serogroup 1 lipopolysaccharide biosynthesis gene cluster (MIBiG accession:

BGC0000775)(Lüneberg et al., 2000; Medema et al., 2015). Ten percent of the genes of the gene clusters show similarity with the *Burkholderia pseudomallei* type II O-antigen biosynthesis gene cluster (MIBiG accession: BGC0000782)(DeShazer et al., 1998). Based on these results, we speculate that the serovar-specific gene cluster was O-antigen biosynthesis gene cluster of *R. anatipestifer*.

We further compared the distribution of the gene cluster between different serotypes, and the results showed that the position of the gene cluster was relatively conserved in the genome of *R. anatipestifer* (Figure 1). In short, the gene region has conserved fragments of 4 and 5 genes (excluding the border) at the beginning and end, respectively (Figure 2).

Analysis of O-antigen gene cluster

To determine the boundaries of the O-antigen gene cluster, we focused on the locations where those O-antigen synthesis genes were densely located. Meanwhile, we reviewed the aforementioned lipopolysaccharide biosynthetic gene clusters, which were conserved in *R. anatipestifer*. Both antiSMASH and DeepBGC characterize a BGC at positions 908750--941443 (RA-CH-2, CP004020.1). According to the antiSMASH results, 10% of the genes in this BGC and the O-antigen gene cluster (GenBank accession: AF064070.1) show similarity. Interestingly, there is a dividing line around the distribution of genes involved in O-antigen synthesis near this area (Figure 3). Several other serotypes had the same situation (Supplementary Figure 1).

Therefore, we speculated that the O-antigen gene cluster of RA-CH-2 was

located between *recX* (recombinase, Accession No. G148_RS04315) and *rimO* (ribosomal protein S12 methylthiotransferase, Accession No. G148_RS04430), both of which were highly conserved in *R. anatipestifer*.

The O-antigen gene cluster of RA-CH-2 was 25.6 kb, and the G + C content was 34.00%. It included 22 open reading frames (ORFs) with the same transcriptional direction (Figure 5). To assign annotations the genes, BLAST searches against the NR database and CDD were performed (Table 3).

Generally, the coding sequence within O-antigen gene clusters primarily consists of the following three categories: nucleotide sugar biosynthesis, glycosyl transferase, and O-antigen processing(Kalynych et al., 2014). Among gram-negative bacteria, O-antigen processing enzymes include a flippase (Wzx) and O-antigen polymerase (Wzy), which are involved in the transmembrane transport of O-units and the synthesis of O-antigens, respectively(Kalynych et al., 2014). It is worth noting that *wzx* and *wzy* are usually used as serotype molecular detection targets due to their serotype specificity.

To analyse the oligosaccharide unit processing genes, we used TMHMM2.0 to predict the transmembrane domains in the proteins. The results showed that *G148_RS04350* and *G148_RS04365* contain multiple transmembrane regions (Figure 4). A 50 amino acid stem-loop structure is located between the second and third transmembrane regions (Figure 4 b).The large stem-loop structure distributed in the periplasmic region is a typical feature of the O-antigen polymerase (Wzy)(Daniels et

al., 1998). Furthermore, the protein of *G148_RS04365* shared 23.41% identity, 45.55% similarity and 86.40% coverage with Wzy (ACD37078.1) from *Shigella boydii* (Table 3).

The protein encoded by *G148_RS04350* contains 14 uniformly distributed transmembrane regions (Figure 4 a). *G148_RS04350* shows 33.01% identity, 53.11% similarity and 85.95% coverage to the O-unit flippase (ABG81799.1, AJR19423.1) in *E. coli* and 32.67% identity, 52.32% similarity and 92.35% coverage to the O-unit flippase in *Providencia alcalifaciens*. The set of *wzx* and *wzy* genes suggests the presence of Wzx/Wzy pathway related O-antigen processing.

Inter- and intra-serotypes comparison of O-AGCs

Based on the positional conservation of the O-antigen gene cluster, we extracted the O-antigen gene cluster sequences from other strains (34 strains，Supplementary Table 4). The length of the gene clusters from 20.22 kb (RCAD0135) to 28.38 kb (RCAD0179), GC content between 32.26% (CCUG25011) and 34.00% (RCAD0123), which was significantly lower than the GC content of the genome (upper quartile: 35.05%, lower quartile: 34.97%, mean: 35.00%; Wilcoxon test: p-value = 5.476e-16). These gene clusters contain an average of 25 CDSs (ranging from 20 to 30). We annotated the O-antigen gene clusters of the serotype representative strains marked in Supplementary Table 1, the results are shown in Supplementary Table 5 and Figure 5. It is worth noting that all serotype O-antigen gene clusters contain *wza*, *wzc* and *rmlABC* homologous genes. *rmlABCD* in the serotype 12 gene cluster implies the

possible presence of rhamnose in O-units. The set of *wzx* and *wzy* genes indicates the presence of Wzx/Wzy-related O-antigen processing pathways in the corresponding serotypes.

Next, we extracted the *wzx* and *wzy* gene sequences of all the strains and constructed the NJ phylogenetic tree (Figure 6). The homology matrix of the protein or DNA sequences of the *wxy*, *wzx*, and O-antigen gene clusters was calculated, and the results are shown in Figure 7. Overall, *wzx* and *wzy* are serotype-specific, and much greater differences exist among the different serotypes. Interestingly, RA-YM and RA-GD are reported to be serotype 1(Yuan et al., 2011; Zhou et al., 2011), but their *wzx* and *wzy* are highly identical to our reported serotype 2. CCUG25011 is serotype 4, and *wzx* shares more than 97% similarity with serotype 7. Similarly, CCUG25004 is serotype 5, but *wzy* shares high homology with serotype 2(similarity > 99 %).

In addition, an NJ phylogenetic tree based on the complete sequence of the O-antigen gene cluster and a synteny analysis of the O-antigen gene cluster (DNA sequence identity cut-off: 69%) are shown in Figure 8. As expected, strains of the same serotype clustered into the same clade and had the same gene cluster structure. Consistent with the single gene identification results, the O-antigen gene clusters of RA-YM and RA-GD are highly homologous to the serotype 2 strain. The *wzy* gene of RA-GD is divided into *wzy1* (RIA_1497) and *wzy2* (RIA_1498) according to GenBank. However, the remaining serotype 1 strains were clustered in other clades

and had a consistent genetic structure with each other. Except for a gene insertion event in CCUG25001, the genetic structure of the O-antigen gene cluster of all serotype 2 strains was highly similar (Figure 8). The inserted gene predictive function is O-acetylase involved in peptidoglycan or LPS synthesis (Reference: RBP22008.1; Identity/coverage: 40.95%/99%; E-value: 3e-59). Additionally, CCUG25004 (serotype 5) and the strains of serotype 2 differed by only two genes (Wzx and a glycosyltransferase, Figure 8 and Supplementary Table 5). As expected, serotype 1 strains had identical gene clusters. In contrast to serotype 1, the gene clusters among the serotype 10 strains are more diverse, and even so, their *wxz* and *wxy* are uniform. RCAD0127 and HXb2 have almost the same sequence. Gene clusters in serotype 4 and serotype 7 have high identity, *wzx* is a homologue, but *wxy* is specific (Supplementary Figure 2). Overall, serotype 11 shows reasonable sequence homology.

Conserved loci in other *Flavobacteriaceae* species

The synteny analysis of homologous gene clusters in *Flavobacteriaceae* indicated that the locus of the O-AGC locus was conserved among closely related species (Figure 9a, Supplementary Figure 3). Specifically, the upstream gene arrangement (*recx-gdr-wza-wzc*) of *R. anatipestifer* O-AGCs was highly conserved. *Chryseobacterium* and *R. anatipestifer* were the same (*recx* and *rimO*) at the beginning and end of the region.

As expected, this locus is also conserved in *Elizabethkingia sp.* and

Chryseobacterium sp. (Figure 9b and Figure 9c). Furthermore, many glycosyltransferases related to polysaccharide synthesis are distributed in this region in both genera. It is worth mentioning that *rmlABC* (*Elizabethkingia sp.*), lipopolysaccharide export system ATP-binding protein gene (*lptB, Elizabethkingia sp.*), O-antigen ligase gene (*Chryseobacterium sp.*), and oligosaccharide flippase gene (*Chryseobacterium sp.*) were also present in the conserved region, and they are usually involved in the synthesis of O-antigen or lipopolysaccharide.

Regarding the other two species of *Riemerella*: *Riemerella columbina* and *Riemerella columbipharyngis*, a similar gene cluster was found in *Riemerella columbina* DSM 16469 (Supplementary Figure 4). Furthermore, the genes encoding oligosaccharide repeat unit polymerase (Wzy) and oligosaccharide flippase (Wzx) were annotated in the cluster. However, compared with *Riemerella anatipestifer* RA-CH-2 O-AGCs, the cluster region is significantly rearranged in *Riemerella columbina*. Unfortunately, due to a lack of data, we could not detect similar genetic regions in *Riemerella columbipharyngis*.

Multiplex serotyping PCR of *R. anatipestifer* serotype 1, 2 and 11

Based on comparative analysis of the inter- and intra-serotypes, we identified specific sites for the three major serotypes. A multiplex PCR method was developed for molecular serotyping (Table 2 and Figure 10). For *R. anatipestifer* serotypes 1,2 and 11, serotyping PCR can produce bands of the correct size for serotyping and species identification (Figure 10a). For the other serotypes (3, 4, 5, 6, 7, 8, 10 and 12),

PCR only amplified the species's identification band (Figure 10c). Moreover, our method has high specificity for common avian pathogens. Even *Riemerella columbina*, belongs to the same genus as *R. anatipestifer* (Figure 10b).

To evaluate the performance of mPCR, we tested 181 serotype known isolates (n=45, serotype 1; n=79, serotype 2; n=49, serotype 11; n=8, other serotypes). Compared to the agglutination typing method, the coincidence rates of mPCR for serotypes 1, 2 and 11 were 93.33% (42/45), 97.47% (77/79) and 100% (49/49), respectively. An excellent agreement was found between the mPCR and the agglutination method, with kappa index 0.96±0.03 at the 95% confidence level (*p*-value < 2.2e-16).

Identification and agglutination characterization of *R. anatipestifer* CH-2Δ*wzy*

The *wzy* of *R. anatipestifer* CH-2 was knocked out by allelic exchange, and the mutant CH-2Δ*wzy* was identified by PCR(Figure 1). CH-2Δ*wzy* amplified the 16S rRNA fragment, $Spec^R$ cassette fragment, and LSR fragment, but did not amplify the *wzy* fragment. All amplicons were confirmed by Sanger sequencing. After continuous culture for 30 generations, the genetic stability of the CH-2Δ*wzy* mutant was confirmed by the same PCR test. A standard antisera slide agglutination test showed that CH-2Δ*wzy* could not agglutinate with the antisera of serotype 2 (Figure 13).

Discussion

In the present study, we used Pan-GWAS and identified the genetic loci significantly associated with *R. anatipestifer* serotype 1, serotype 2, serotype 10 and

serotype 11. Further functional analysis of the loci suggested that these genes are responsible for the synthesis of O-antigen-related polysaccharides. This is consistent with previous studies showing that each serotype of gram-negative bacterial species corresponds to a specific cluster of O-antigen synthesis genes(Aydanian et al., 2011; Kenyon et al., 2017; Liu et al., 2014; Liu et al., 2008; Seif et al., 2019; Wang et al., 2017b). Wang et al. mutated the *AS87_04050* gene (strain Yb2, serotype 2) located in the abovementioned O-antigen gene cluster. The results showed that compared with the wild-type strain, the mutant LPS was defective and lost it's agglutination ability to serotype 2-positive antisera(Wang et al., 2014). Similarly, Zou et al. mutated the *M949_1603* gene in the above gene cluster in *R. anatipestifer* CH-3 and found that the LPS of the mutant strain lacks the O-antigen chain(Zou et al., 2015). Two other studies reported similar results, that is, the expression of *M949_RS07580* was significantly downregulated in the CH-3 mutant strain, which lacks O-antigen repeat units(Dou et al., 2017; Dou et al., 2018). *M949_RS07580* is also located in the O-antigen gene cluster.

Based on the results of the correlation study between serotype and genome, we predicted and analysed the O-antigen gene cluster of *R. anatipestifer*. The existence of *wzx* and *wzy* means that the O-antigen polysaccharide units are assembled via the Wzx/Wzy-dependent pathway. Functional annotation predicted that the *G148_RS04365* gene of *R. anatipestifer* CH-2 was *wzy* (coding O-antigen polymerase, Wzy; Table 3). *G148_RS04365* protein contains contain 10 transmembrane regions,

which is the basic characteristic of Wzy. Furthermore, the *wzy* gene (G148_RS04365) was deleted from *R. anatipestifer* CH-2, and the mutant CH-2Δ*wzy* could not agglutinate with antisera of serotype 2, which indicates that the mutant strain antigen was defective. The same phenomenon occurred in Yb2 when the *AS87_04050* gene (predicted nucleoside-diphosphate-sugar epimerase) was knocked out(Wang et al., 2014).The above results also indicate that the O-antigen gene cluster our proposed is closely related to the serotype of *R. anatipestifer*.

In this study, we performed a conservative analysis of the O-AGCs of *R. anatipestifer* in *Flavobacterium* species. It is noteworthy that a similar genetic locus is harboured in some species of *Chryseobacterium* and *Elizabethkingia* (Figure 9). However, there have been no reports about the O-antigen gene cluster of *Chryseobacterium* and *Elizabethkingia*. Despite this limitation, we found several genes related to O-antigen synthesis in these regions, such as *wbpA*, *wbpD*, *wbpE*, *lptB* and the ABC transporter ATP-binding protein gene(Luo et al., 2017; Shoji et al., 2014). Therefore, for some species of *Chryseobacterium* and *Elizabethkingia*, the abovementioned genomic region may also be the locus of the O-antigen gene cluster.

The comparison of the O-AGCs of a total of 11 serotypes indicates that the O-AGC of *R. anatipestifer* is conserved at both ends and variable in the middle region (Figure 8). Similar phenomena also appeared in *Plesiomonas shigelloides*(Xi et al., 2019), *Escherichia albertii*(Wang et al., 2017b), and *Yersinia pseudotuberculosis*(Kenyon et al., 2017). Variations in the O-AGCs often mean

differences in the O-antigen oligosaccharide unit and affect the serological phenotype. Our analysis of the phylogenetic relationship of the O-AGCs from *R. anatipestifer*'s 11 serotypes (38 strains) reveals correspondence between the O-AGCs and their serotypes. In the present study, mPCR based on specific sequence for each serotype to detect three main serotypes was developed. To evaluate the performance of the mPCR method, we compared it with standard slide agglutination serotyping, and the results show that agreement between our method and conventional agglutination methods was very high (kappa = 0.96±0.03), which indicates that the mPCR method could be an alternative to the traditional method. Since first using slide agglutination test to determine serotypes of *R. anatipestifer*(Bisgaard, 1982), no new molecular serotyping scheme has been proposed to conveniently detect the serotype. Therefore, our findings and proposed method were significant for the establishment of system serotyping schemes for *R. anatipestifer*.

Conclusion

In this work, we revealed that the serotype of *R. anatipestifer* is related to the putative O-antigen gene cluster through a genome-wide association studies and construction of a gene knockout strain. We characterized the O-antigen gene clusters of 11 of *R. anatipestifer* serotypes and demonstrated their genetic diversity. The serotyping mPCR approach defined here will facilitate work on the epidemiological surveillance of *R. anatipestifer*.

Funding

This work was supported by Sichuan Science and Technology Program (2020YJ0330); Sichuan Veterinary Medicine and Drug Innovation Group of China Agricultural Research System (SCCXTD-2021-18); China Agriculture Research System of MOF and MARA.

References

Aydanian, A., Tang, L., Morris, J.G., Johnson, J.A., Stine, O.C., 2011. Genetic diversity of O-antigen biosynthesis regions in Vibrio cholerae. Applied and environmental microbiology 77, 2247-2253.

Bian, S., Zeng, W., Li, Q., Li, Y., Wong, N.K., Jiang, M., Zuo, L., Hu, Q., Li, L., 2020. Genetic Structure, Function, and Evolution of Capsule Biosynthesis Loci in Vibrio parahaemolyticus. Frontiers in microbiology 11, 546150.

Bisgaard, M., 1982. Antigenic studies on Pasteurella anatipestifer, species incertae sedis, using slide and tube agglutination. Avian Pathology 11, 341-350.

Blin, K., Wolf, T., Chevrette, M.G., Lu, X., Schwalen, C.J., Kautsar, S.A., Suarez Duran, H.G., de Los Santos, E.L.C., Kim, H.U., Nave, M., Dickschat, J.S., Mitchell, D.A., Shelest, E., Breitling, R., Takano, E., Lee, S.Y., Weber, T., Medema, M.H., 2017. antiSMASH 4.0-improvements in chemistry prediction and gene cluster boundary identification. Nucleic acids research 45, W36-W41.

Boulianne, M., Blackall, P.J., Hofacre, C.L., Ruiz, J.A., Sandhu, T.S., Hafez, H.M., Chin, R.P., Register, K.B., Jackwood, M.W. Riemerella anatipestifer Infection, In: Diseases of Poultry. 846-853.

Brynildsrud, O., Bohlin, J., Scheffer, L., Eldholm, V., 2016. Rapid scoring of genes in microbial pan-genome-wide association studies with Scoary. Genome biology 17, 238.

Carter, G.R., 1955. Studies on Pasteurella multocida. I. A hemagglutination test for the identification of serological types. Journal of Veterinary Research 16, 481-484.

450 Daniels, C., Vindurampulle, C., Morona, R., 1998. Overexpression and topology of
451 the Shigella flexneri O-antigen polymerase (Rfc/Wzy). Molecular microbiology
452 28, 1211-1222.
453 DeShazer, D., Brett, P.J., Woods, D.E., 1998. The type II O-antigenic polysaccharide
454 moiety of Burkholderia pseudomallei lipopolysaccharide is required for serum
455 resistance and virulence. Molecular microbiology 30, 1081-1100.
456 Dou, Y., Wang, X., Yu, G., Wang, S., Tian, M., Qi, J., Li, T., Ding, C., Yu, S., 2017.
457 Disruption of the M949_RS01915 gene changed the bacterial lipopolysaccharide
458 pattern, pathogenicity and gene expression of Riemerella anatipestifer. Veterinary
459 research 48, 6.
460 Dou, Y., Yu, G., Wang, X., Wang, S., Li, T., Tian, M., Qi, J., Ding, C., Yu, S., 2018.
461 The Riemerella anatipestifer M949_RS01035 gene is involved in bacterial
462 lipopolysaccharide biosynthesis. Veterinary research 49, 93.
463 Edwards, R.A., Keller, L.H., Schifferli, D.M., 1998. Improved allelic exchange
464 vectors and their use to analyze 987P fimbria gene expression. Gene 207,
465 149-157.
466 Fang, C.T., Shih, Y.J., Cheong, C.M., Yi, W.C., 2016. Rapid and Accurate
467 Determination of Lipopolysaccharide O-Antigen Types in Klebsiella pneumoniae
468 with a Novel PCR-Based O-Genotyping Method. Journal of Clinical
469 Microbiology 54, 666-675.
470 Farhat, M.R., Freschi, L., Calderon, R., Ioerger, T., Snyder, M., Meehan, C.J., de Jong,
471 B., Rigouts, L., Sloutsky, A., Kaur, D., 2019. GWAS for quantitative resistance
472 phenotypes in Mycobacterium tuberculosis reveals resistance genes and
473 regulatory regions. Nature communications 10, 1-11.
474 Franklin, K., Lingohr, E.J., Yoshida, C., Anjum, M., Bodrossy, L., Clark, C.G.,
475 Kropinski, A.M., Karmali, M.A., 2011. Rapid Genoserotyping Tool for
476 Classification of Salmonella Serovars. Journal of Clinical Microbiology 49,
477 2954-2965.

478 Hannigan, G.D., Prihoda, D., Palicka, A., Soukup, J., Klempir, O., Rampula, L.,
479 Durcak, J., Wurst, M., Kotowski, J., Chang, D., Wang, R., Piizzi, G., Temesi, G.,
480 Hazuda, D.J., Woelk, C.H., Bitton, D.A., 2019. A deep learning genome-mining
481 strategy for biosynthetic gene cluster prediction. Nucleic acids research 47, e110.
482 Iguchi, A., Nishii, H., Seto, K., Mitobe, J., Lee, K., Konishi, N., Obata, H., Kikuchi,
483 T., Iyoda, S., 2020. Additional Og-typing PCR techniques targeting E. coli-novel
484 and Shigella-unique O-antigen biosynthesis gene clusters. Journal of Clinical
485 Microbiology 58, e01493-01420.
486 Kalynych, S., Morona, R., Cygler, M., 2014. Progress in understanding the assembly
487 process of bacterial O-antigen. FEMS microbiology reviews 38, 1048-1065.
488 Katoh, K., Misawa, K., Kuma, K.i., Miyata, T., 2002. MAFFT: a novel method for
489 rapid multiple sequence alignment based on fast Fourier transform. Nucleic acids
490 research 30, 3059-3066.
491 Kenyon, J.J., Cunneen, M.M., Reeves, P.R., 2017. Genetics and evolution of Yersinia
492 pseudotuberculosis O-specific polysaccharides: a novel pattern of O-antigen
493 diversity. FEMS microbiology reviews 41, 200-217.
494 Krogh, A., Larsson, B., Von Heijne, G., Sonnhammer, E.L., 2001. Predicting
495 transmembrane protein topology with a hidden Markov model: application to
496 complete genomes. Journal of molecular biology 305, 567-580.
497 Kumar, S., Stecher, G., Tamura, K., 2016. MEGA7: molecular evolutionary genetics
498 analysis version 7.0 for bigger datasets. Molecular biology and evolution 33,
499 1870-1874.
500 Leclercq, R., Courvalin, P., 1991. Bacterial resistance to macrolide, lincosamide, and
501 streptogramin antibiotics by target modification. Antimicrob Agents Chemother
502 35, 1267-1272.
503 Li, W., Godzik, A., 2006. Cd-hit: a fast program for clustering and comparing large
504 sets of protein or nucleotide sequences. Bioinformatics 22, 1658-1659.
505 Liao, H.B., Cheng, X.J., Zhu, D.K., Wang, M.S., Jia, R.Y., Chen, S., Chen, X.Y.,

506 Biville, F., Liu, M.F., Cheng, A.C., 2015. TonB Energy Transduction Systems of
507 Riemerella anatipestifer Are Required for Iron and Hemin Utilization. Plos One
508 10, e0127506.
509 Liu, B., Furevi, A., Perepelov, A.V., Guo, X., Cao, H., Wang, Q., Reeves, P.R., Knirel,
510 Y.A., Wang, L., Widmalm, G., 2020. Structure and genetics of Escherichia coli O
511 antigens. FEMS microbiology reviews 44, 655-683.
512 Liu, B., Knirel, Y.A., Feng, L., Perepelov, A.V., Senchenkova, S.N., Reeves, P.R.,
513 Wang, L., 2014. Structural diversity in Salmonella O antigens and its genetic
514 basis. FEMS microbiology reviews 38, 56-89.
515 Liu, B., Knirel, Y.A., Feng, L., Perepelov, A.V., Senchenkova, S.N., Wang, Q., Reeves,
516 P.R., Wang, L., 2008. Structure and genetics of Shigella O antigens. FEMS
517 microbiology reviews 32, 627-653.
518 Lüneberg, E., Zetzmann, N., Alber, D., Knirel, Y.A., Kooistra, O., Zähringer, U.,
519 Frosch, M., 2000. Cloning and functional characterization of a 30 kb gene locus
520 required for lipopolysaccharide biosynthesis in Legionella pneumophila.
521 International journal of medical microbiology 290, 37-49.
522 Luo, H., Liu, M., Wang, L., Zhou, W., Wang, M., Cheng, A., Jia, R., Chen, S., Sun, K.,
523 Yang, Q., Chen, X., Zhu, D., 2015. Identification of ribosomal RNA
524 methyltransferase gene ermF in Riemerella anatipestifer. Avian Pathology 44,
525 162-168.
526 Luo, Q., Yang, X., Yu, S., Shi, H., Wang, K., Xiao, L., Zhu, G., Sun, C., Li, T., Li, D.,
527 Zhang, X., Zhou, M., Huang, Y., 2017. Structural basis for lipopolysaccharide
528 extraction by ABC transporter LptB2FG. Nature Structural & Molecular Biology
529 24, 469-474.
530 Ma, K.C., Mortimer, T.D., Duckett, M.A., Hicks, A.L., Wheeler, N.E., Sánchez-Busó,
531 L., Grad, Y.H., 2020. Increased power from conditional bacterial genome-wide
532 association identifies macrolide resistance mutations in Neisseria gonorrhoeae.
533 Nature communications 11, 1-8.

534 Marchler-Bauer, A., Derbyshire, M.K., Gonzales, N.R., Lu, S., Chitsaz, F., Geer, L.Y.,
535 Geer, R.C., He, J., Gwadz, M., Hurwitz, D.I., 2014. CDD: NCBI's conserved
536 domain database. Nucleic acids research 43, D222-D226.
537 Medema, M.H., Kottmann, R., Yilmaz, P., Cummings, M., Biggins, J.B., Blin, K., De
538 Bruijn, I., Chooi, Y.H., Claesen, J., Coates, R.C., 2015. Minimum information
539 about a biosynthetic gene cluster. Nature chemical biology 11, 625.
540 Medema, M.H., Takano, E., Breitling, R., 2013. Detecting sequence homology at the
541 gene cluster level with MultiGeneBlast. Molecular biology and evolution 30,
542 1218-1223.
543 Page, A.J., Cummins, C.A., Hunt, M., Wong, V.K., Reuter, S., Holden, M.T., Fookes,
544 M., Falush, D., Keane, J.A., Parkhill, J., 2015. Roary: rapid large-scale
545 prokaryote pan genome analysis. Bioinformatics 31, 3691-3693.
546 Pathanasophon, P., Phuektes, P., Tanticharoenyos, T., Narongsak, W., Sawada, T.,
547 2002. A potential new serotype of Riemerella anatipestifer isolated from ducks in
548 Thailand. Avian Pathology 31, 267-270.
549 Qu, W., Zhang, C. 2015. Selecting specific PCR primers with MFEprimer, In: PCR
550 Primer Design. Springer, 201-213.
551 Saitou, N., Nei, M., 1987. The neighbor-joining method: a new method for
552 reconstructing phylogenetic trees. Molecular biology and evolution 4, 406-425.
553 Seemann, T., 2014. Prokka: rapid prokaryotic genome annotation. Bioinformatics 30,
554 2068-2069.
555 Seif, Y., Monk, J.M., Machado, H., Kavvas, E., Palsson, B.O., 2019. Systems Biology
556 and Pangenome of Salmonella O-Antigens. mBio 10, e01247-01219.
557 Shoji, M., Sato, K., Yukitake, H., Naito, M., Nakayama, K., 2014. Involvement of the
558 Wbp pathway in the biosynthesis of Porphyromonas gingivalis
559 lipopolysaccharide with anionic polysaccharide. Scientific reports 4, 5056.
560 Sullivan, M.J., Petty, N.K., Beatson, S.A., 2011. Easyfig: a genome comparison
561 visualizer. Bioinformatics 27, 1009-1010.

562 Townsend, K.M., Boyce, J.D., Chung, J.Y., Frost, A.J., Adler, B., 2001. Genetic
563 organization of Pasteurella multocida cap Loci and development of a multiplex
564 capsular PCR typing system. Journal of Clinical Microbiology 39, 924-929.
565 Wang, H., Zheng, H., Li, Q., Xu, Y., Wang, J., Du, P., Li, X., Liu, X., Zhang, L., Zou,
566 N., 2017a. Defining the genetic features of O-antigen biosynthesis gene cluster
567 and performance of an O-antigen serotyping scheme for Escherichia albertii.
568 Frontiers in microbiology 8, 1857.
569 Wang, H., Zheng, H., Li, Q., Xu, Y., Wang, J., Du, P., Li, X., Liu, X., Zhang, L., Zou,
570 N., Yan, G., Zhang, Z., Jing, H., Xu, J., Xiong, Y., 2017b. Defining the Genetic
571 Features of O-Antigen Biosynthesis Gene Cluster and Performance of an
572 O-Antigen Serotyping Scheme for Escherichia albertii. Frontiers in microbiology
573 8, 1857.
574 Wang, X., Ding, C., Wang, S., Han, X., Hou, W., Yue, J., Zou, J., Yu, S., 2014. The
575 AS87_04050 gene is involved in bacterial lipopolysaccharide biosynthesis and
576 pathogenicity of Riemerella anatipestifer. PloS one 9, e109962.
577 Xi, D., Wang, X., Ning, K., Liu, Q., Jing, F., Guo, X., Cao, B., 2019. O-antigen gene
578 clusters of Plesiomonas shigelloides serogroups and its application in
579 development of a molecular serotyping scheme. Frontiers in microbiology 10,
580 741.
581 Young, B.C., Earle, S.G., Soeng, S., Sar, P., Kumar, V., Hor, S., Sar, V., Bousfield, R.,
582 Sanderson, N.D., Barker, L., 2019. Panton–Valentine leucocidin is the key
583 determinant of Staphylococcus aureus pyomyositis in a bacterial GWAS. Elife 8,
584 e42486.
585 Yuan, J., Li, Y.-Y., Xu, Y., Sun, B.-J., Shao, J., Zhang, D., Li, K., Fan, D.-D., Xue,
586 Z.-B., Chen, W.-H., 2019. Molecular Signatures Related to the Virulence of
587 Bacillus cereus Sensu Lato, a Leading Cause of Devastating Endophthalmitis.
588 mSystems 4, e00745-00719.
589 Yuan, J., Liu, W., Sun, M., Song, S., Cai, J., Hu, S., 2011. Complete genome sequence

of the pathogenic bacterium Riemerella anatipestifer strain RA-GD. Journal of bacteriology 193, 2896-2897.

Zankari, E., Hasman, H., Kaas, R.S., Seyfarth, A.M., Agersø, Y., Lund, O., Larsen, M.V., Aarestrup, F.M., 2013. Genotyping using whole-genome sequencing is a realistic alternative to surveillance based on phenotypic antimicrobial susceptibility testing. Journal of antimicrobial chemotherapy 68, 771-777.

Zeng, X., Chi, X., Ho, B.T., Moon, D., Lambert, C., Hall, R.J., Baybayan, P., Wang, S., Wilson, B.A., Ho, M., 2019. Comparative Genome Analysis of an Extensively Drug-Resistant Isolate of Avian Sequence Type 167 Escherichia coli Strain Sanji with Novel In Silico Serotype O89b:H9. mSystems 4, e00242-00218.

Zhou, Z., Peng, X., Xiao, Y., Wang, X., Guo, Z., Zhu, L., Liu, M., Jin, H., Bi, D., Li, Z., Sun, M., 2011. Genome sequence of poultry pathogen Riemerella anatipestifer strain RA-YM. Journal of bacteriology 193, 1284-1285.

Zou, J., Wang, X., Ding, C., Tian, M., Han, X., Wang, S., Yu, S., 2015. Characterization and cross-protection evaluation of M949_1603 gene deletion Riemerella anatipestifer mutant RA-M1. Applied microbiology and biotechnology 99, 10107-10116.

Figure legends

Figure 1. Location of genes significantly associated with serotypes. And the specificity and the sensitivity of genes significantly associated with Serotype 1, 2, 10 and 11. The size of the shape indicates sensitivity; colour indicates negative value of *P*-value (adjusted).

Figure 2. Comparison of serotype-associated regions.

Figure 3. CH-2 O-antigen gene cluster location and boundary determination. The dot plot represents the hits of genes related to O-antigen synthesis on the genome,

and the size of the dot indicates the coverage length. Interval markers on gene clusters indicate the BGC regions predicted by DeepBGC and antiSMASH.

Figure 4. The prediction of transmembrane helices in amino acid sequences encoded by *wzx* and *wzy*. a) The prediction of transmembrane helices in the amino acid sequence encoded by *G148_RS04350*. b) The prediction of transmembrane helices in the amino acid sequence encoded by *G148_RS04365*.

Figure 5. The O-antigen gene cluster in *R. anatipestifer* serotypes 1, 3, 4, 5, 6, 7, 9, 10, 11 and 12

Figure 6. Phylogenetic tree constructed by the neighbor joining method based on the *wzx* (a) and *wzy* (b) genes. Numbers in the outer circle indicate serotypes.

Figure 7. *wzx* and *wzy* homology matrix calculated by DNAMAN. The value in front of the strain ID indicates the serotype. a) Protein homology matrix encoded by the *wzx* gene. b) Homology matrix of the *wzx* gene. c) Protein homology matrix encoded by the *wzy* gene. d) Homology matrix of the *wzy* gene.

Figure 8. Neighbor-joining phylogenetic tree and structure of the O-antigen gene cluster. Numbers in boxes indicate serotypes

Figure 9. Conserved loci in other *Flavobacteriaceae* species. a) The genetic locus of the O-antigen gene cluster in *R. anatipestifer* is conserved among the closest species. b) Conserved structure in multiple *Elizabethkingia* species. c) Conserved structure in multiple *Chryseobacterium* species.

Figure 10. Multiplex PCR method for the identification of *R. anatipestifer*

serotypes 1,2 and 11. Lane M, 2000 bp DNA ladder; a) Multiplex PCR method for the identification of *R. anatipestifer* serotypes 1,2 and 11: Lane 1: serotype 1 (ATCC 11845); lane 2: serotype 2 (RA-CH-2); lane 3: serotype 11 (RCAD0147); lane 4: mixed serotypes (1,2,11); and lane 5: Negative control.

b) Detection of species specificity for the multiplex PCR method. Lanes 1 to 4: serotype 1 (ATCC 11845), serotype 2 (RA-CH-2), serotype 11 (RCAD0147), and mixed serotypes (1,2,11); lanes 5 to 8: *Pasteurella multocida*, *Salmonella enterica*, *Riemerella columbina*, *Escherichia coli*; and lane 9: negative control.

c) Detection of serotype specificity for the multiplex PCR method. Lanes 1 to 3: serotype 1 (ATCC 11845), serotype 2 (RA-CH-2) and serotype 11 (RCAD0147); lanes 4 to 11: serotype 3 (CCUG25002), serotype 4 (CCUG25011), serotype 5 (CCUG25004), serotype 6 (CCUG25005), serotype 7 (CCUG25010), serotype 8 (CCUG25054), serotype 10 (RCAD0146) and serotype 12 (CCUG25055); and lane 12: negative control.

Figure 11. Identification of *R. anatipestifer* CH-2Δwzy. M: DL2000 DNA Marker; Lanes 1-3: 16S rRNA F and 16S rRNA R, which amplify a 960 bp fragment from *R. anatipestifer* 16S rRNA. Order: Wild-type(CH-2), mutant(CH-2Δ*wzy*), and negative control (distilled water); Lanes 4-6: Spec F and Spec R, which amplify a 1180 bp fragment from the SpecR cassette. Order: Positive control (pYES1 new), mutant(CH-2Δwzy), and negative control (distilled water); Lanes 7-9: wzy F and wzy R, which amplify an 886 bp fragment from the wzy gene. Order: Wild-type(CH-2),

mutant(CH-2Δ*wzy*), and negative control (distilled water); Lanes 10-11: LSR F and LSR R, which amplify a 1199 bp fragment from the SpecR cassette, indicating that it was inserted in the correct position in the *R. anatipestifer* CH-2 genome. Order: Mutant(CH-2Δ*wzy*), Negative control (distilled water).

Figure 12. Agglutination test of *R. anatipestifer* CH-2Δ*wzy*. a) Wild-type(CH-2) suspension mixed with antisera of serotype 2 ; b) mutant(CH-2Δ*wzy*) suspension mixed with antisera of serotype 2; c) distilled water mixed with antisera of serotype 2; and d) mutant(CH-2Δ*wzy*) suspension mixed with distilled water.

666

667 **Figure**

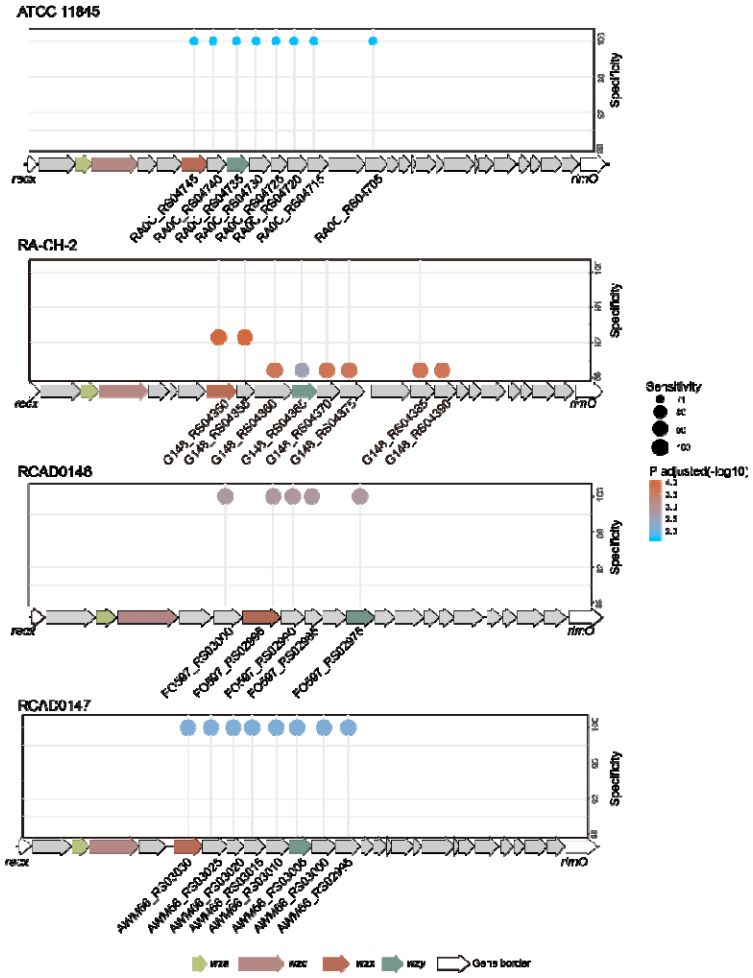

668

669 **Figure 1.** Location of genes significantly associated with serotypes. And the

670 specificity and the sensitivity of genes significantly associated with Serotype 1, 2, 10

671 and 11. The size of the shape indicates sensitivity; colour indicates negative value of

672 *P*-value (adjusted).

673

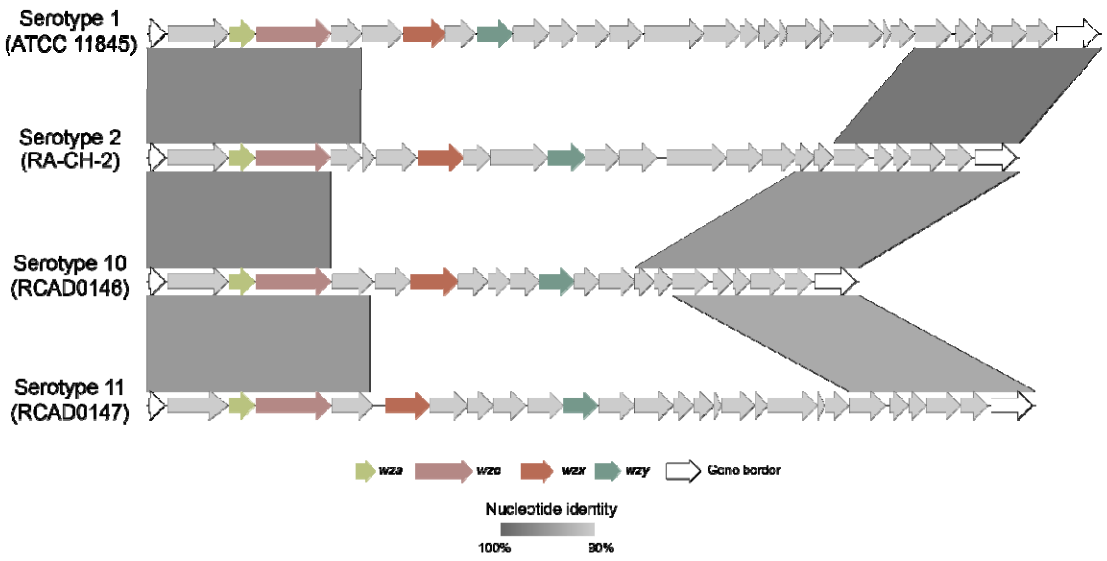

674

675 **Figure 2.** Comparison of serotype-associated regions.

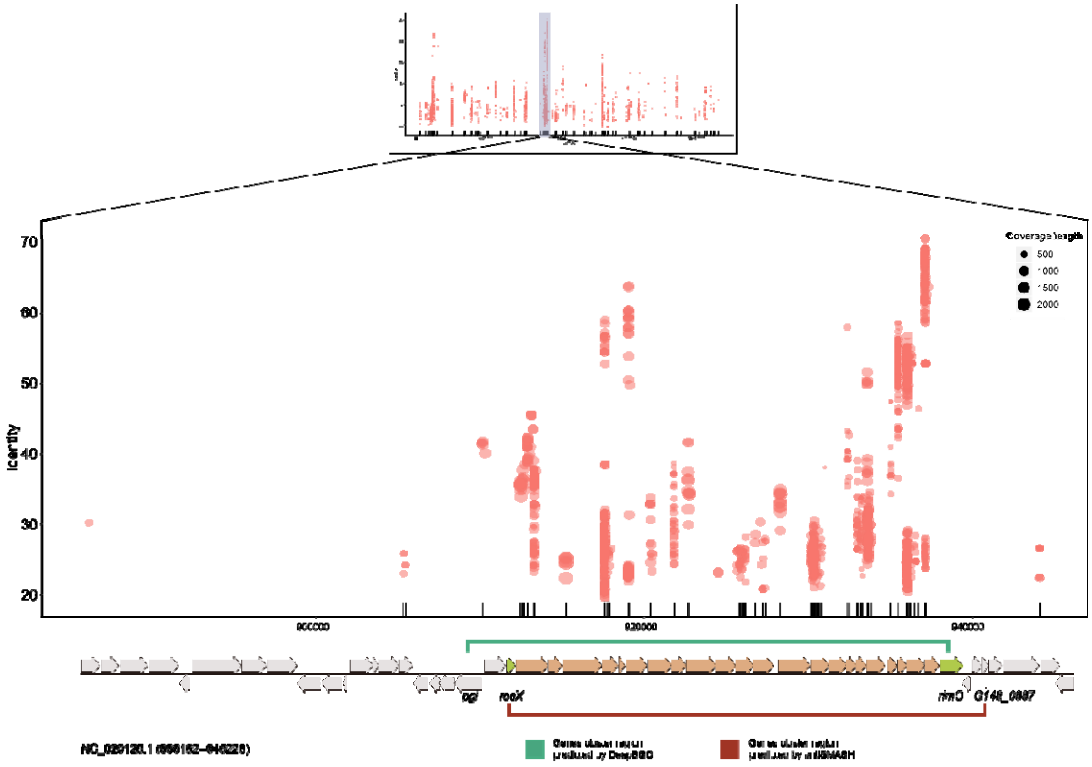

676

677 **Figure 3.** CH-2 O-antigen gene cluster location and boundary determination.

678 The dot plot represents the hits of genes related to O-antigen synthesis on the genome,

679 and the size of the dot indicates the coverage length. Interval markers on gene clusters

680 indicate the BGC regions predicted by DeepBGC and antiSMASH.

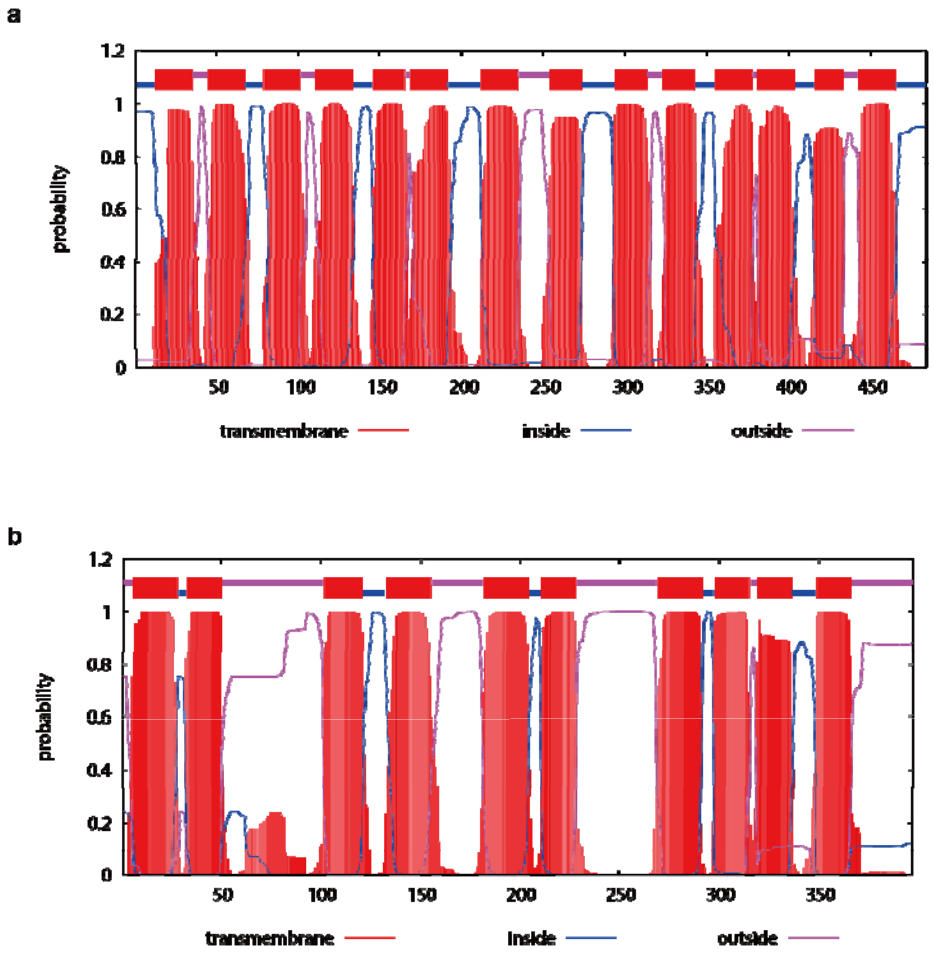

Figure 4. The prediction of transmembrane helices in amino acid sequences encoded by *wzx* and *wzy*. a) The prediction of transmembrane helices in the amino acid sequence encoded by *G148_RS04350*. b) The prediction of transmembrane helices in the amino acid sequence encoded by *G148_RS04365*.

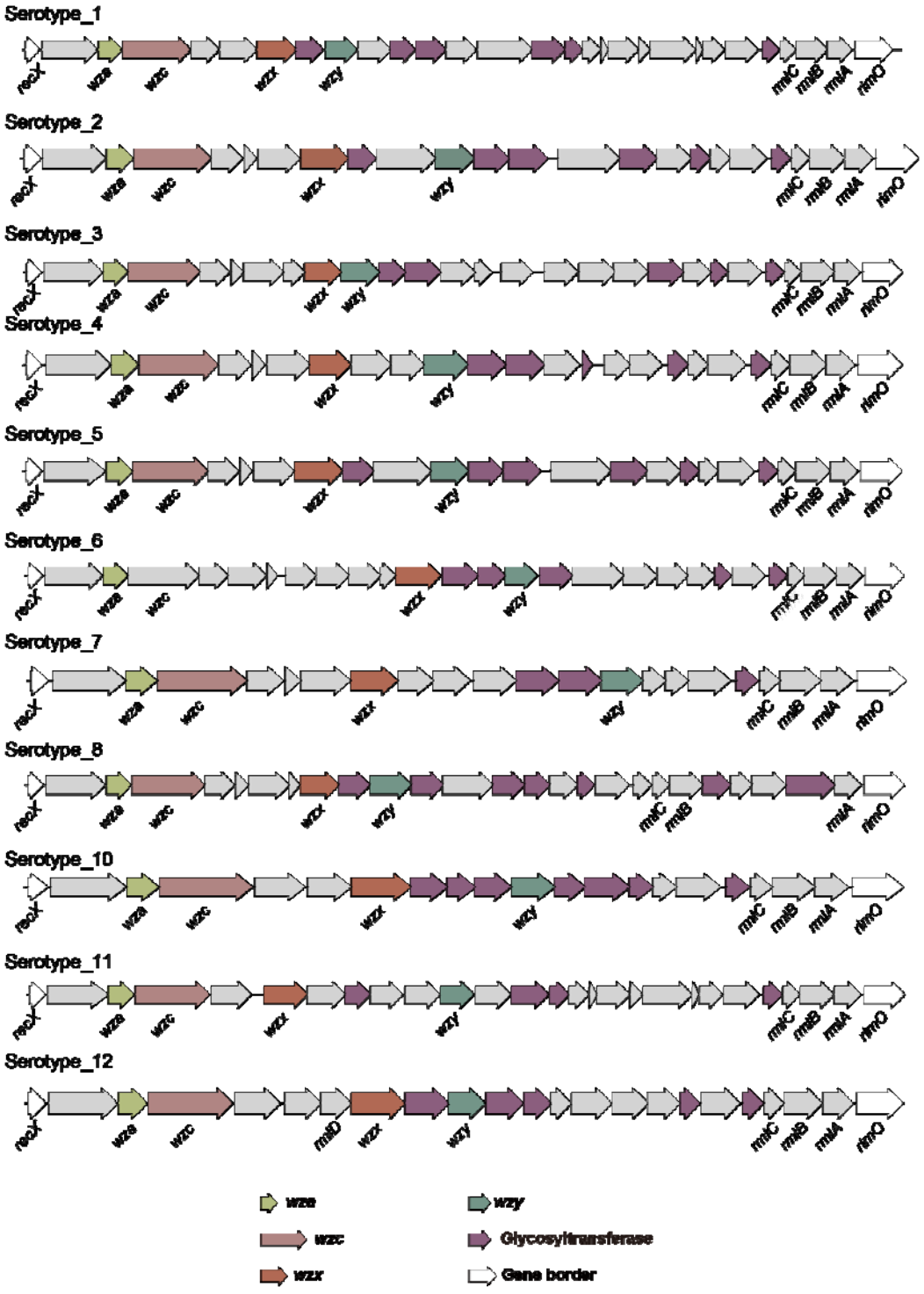

686

687 **Figure 5.** The O-antigen gene cluster in *R. anatipestifer* serotypes 1, 3, 4, 5, 6, 7,

688 9, 10, 11 and 12

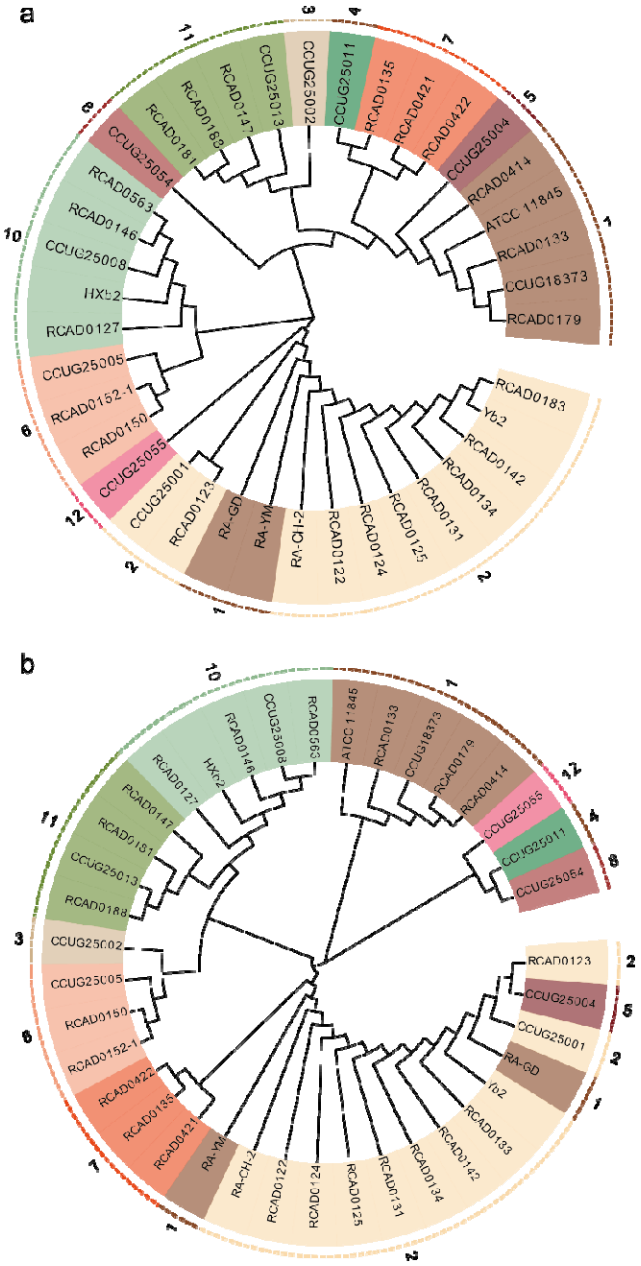

Figure 6. Phylogenetic tree constructed by the neighbor joining method based on the *wzx* (a) and *wzy* (b) genes. Numbers in the outer circle indicate serotypes.

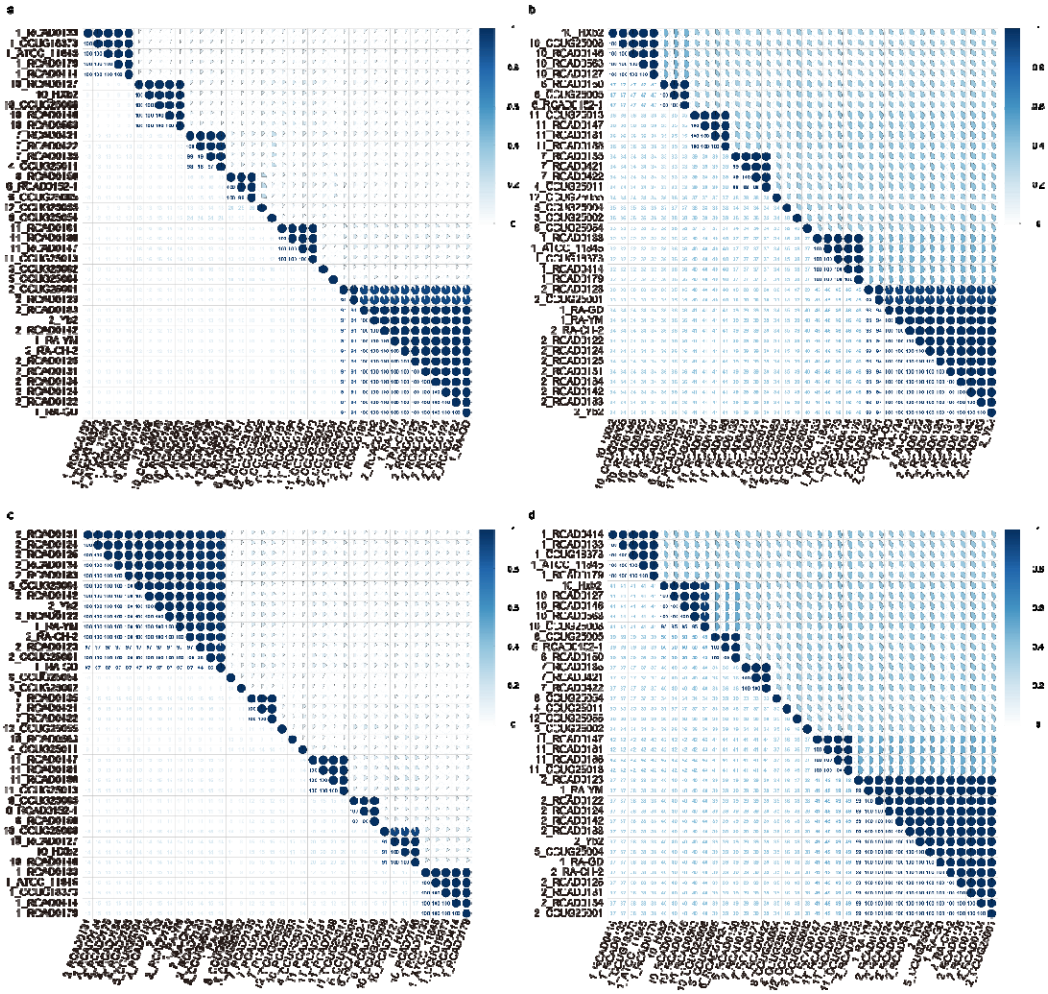

Figure 7. *wzx* and *wzy* homology matrix calculated by DNAMAN. The value in front of the strain ID indicates the serotype. a) Protein homology matrix encoded by the *wzx* gene. b) Homology matrix of the *wzx* gene. c) Protein homology matrix encoded by the *wzy* gene. d) Homology matrix of the *wzy* gene.

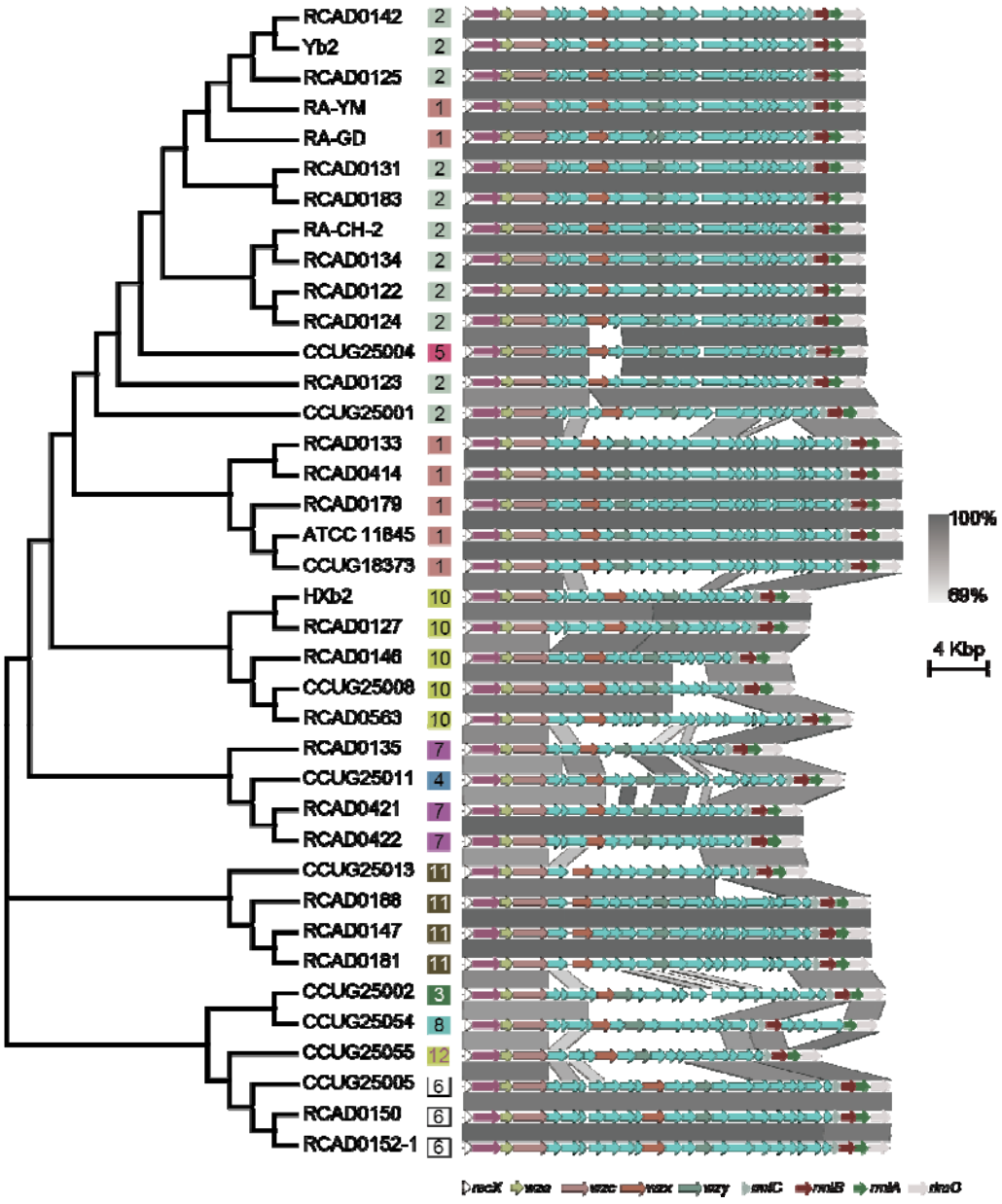

Figure 8. Neighbor-joining phylogenetic tree and structure of the O-antigen gene cluster. Numbers in boxes indicate serotypes

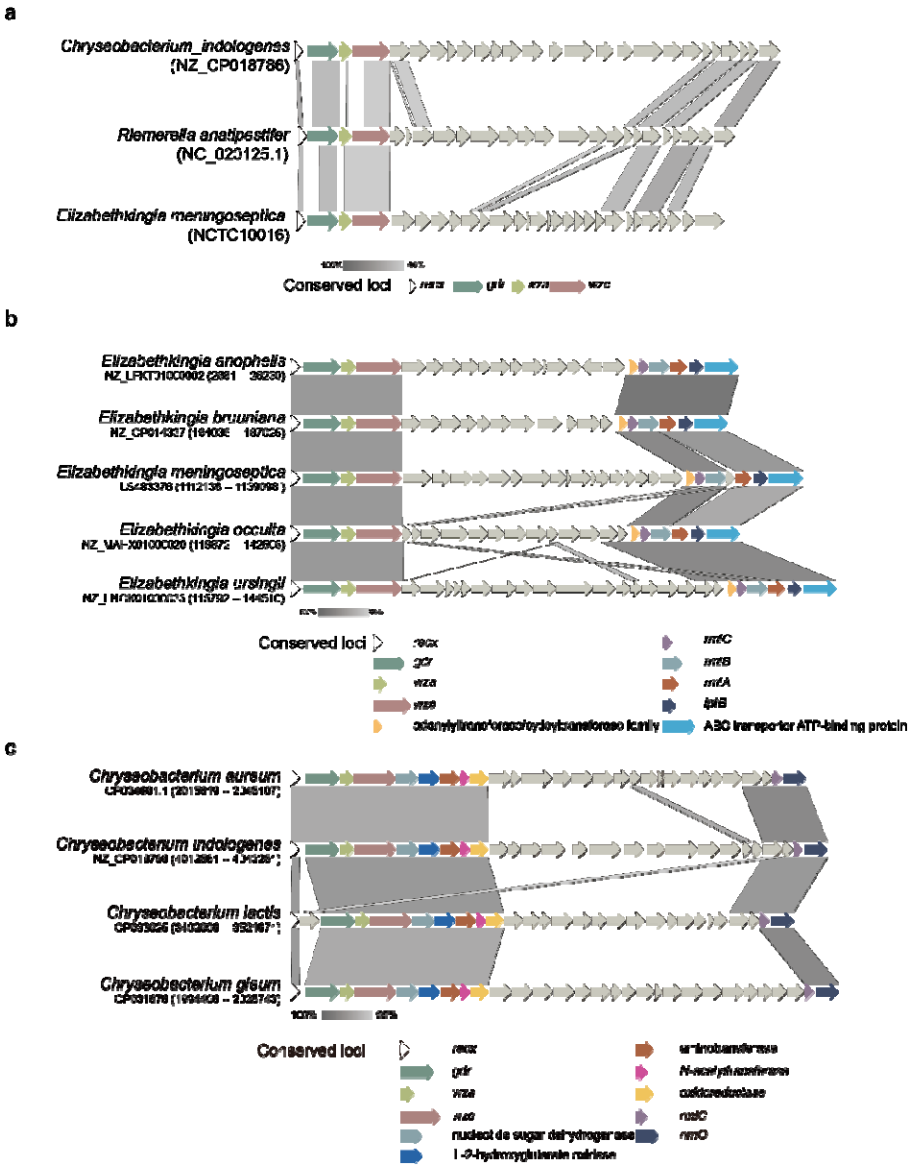

Figure 9. Conserved loci in other *Flavobacteriaceae* species. a) The genetic locus of the O-antigen gene cluster in *R. anatipestifer* is conserved among the closest species. b) Conserved structure in multiple *Elizabethkingia* species. c) Conserved structure in multiple *Chryseobacterium* species.

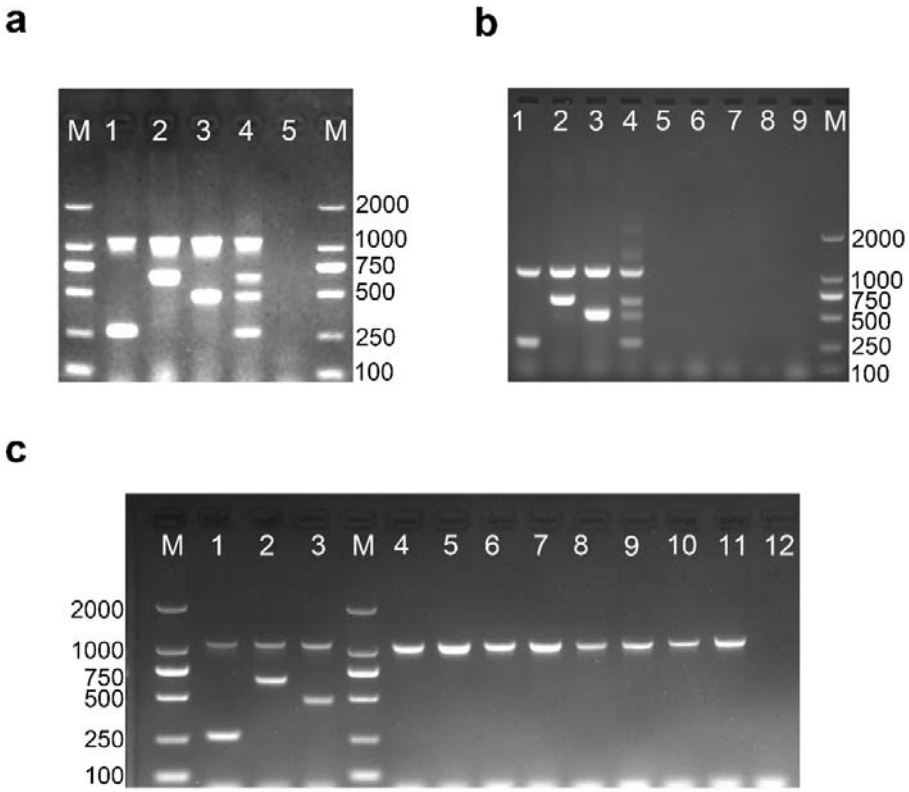

Figure 10. Multiplex PCR method for the identification of *R. anatipestifer* serotypes 1,2 and 11. Lane M, 2000 bp DNA ladder; a) Multiplex PCR method for the identification of *R. anatipestifer* serotypes 1,2 and 11: Lane 1: serotype 1 (ATCC 11845); lane 2: serotype 2 (RA-CH-2); lane 3: serotype 11 (RCAD0147); lane 4: mixed serotypes (1,2,11); and lane 5: Negative control.

b) Detection of species specificity for the multiplex PCR method. Lanes 1 to 4: serotype 1 (ATCC 11845), serotype 2 (RA-CH-2), serotype 11 (RCAD0147), and mixed serotypes (1,2,11); lanes 5 to 8: *Pasteurella multocida*, *Salmonella enterica*, *Riemerella columbina*, *Escherichia coli*; and lane 9: negative control.

c) Detection of serotype specificity for the multiplex PCR method. Lanes 1 to 3: serotype 1 (ATCC 11845), serotype 2 (RA-CH-2) and serotype 11 (RCAD0147);

717 lanes 4 to 11: serotype 3 (CCUG 25002), serotype 4 (CCUG 25011), serotype 5
718 (CCUG 25004), serotype 6 (CCUG 25005), serotype 7 (CCUG 25010), serotype 8
719 (CCUG 25054), serotype 10 (RCAD0146) and serotype 12 (CCUG 25055); and lane
720 12: negative control.
721

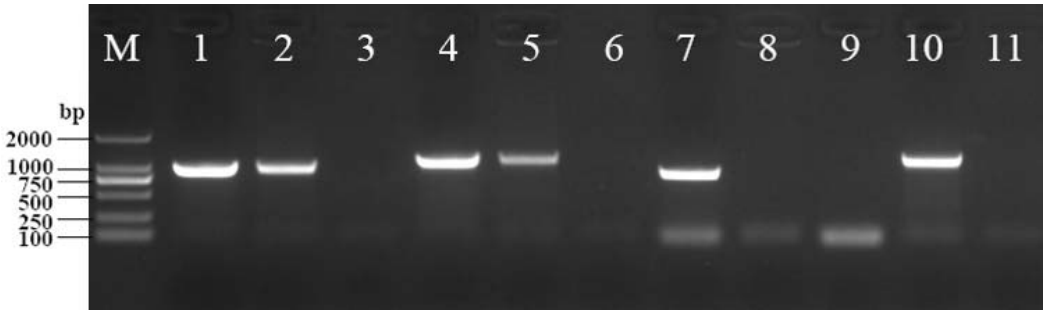

722

723 **Figure 11.** Identification of *R. anatipestifer* CH-2Δwzy. M: DL2000 DNA
724 Marker; Lanes 1-3: 16S rRNA F and 16S rRNA R, which amplify a 960 bp fragment
725 from *R. anatipestifer* 16S rRNA. Order: Wild-type(CH-2), mutant(CH-2Δ*wzy*), and
726 negative control (distilled water); Lanes 4-6: Spec F and Spec R, which amplify a
727 1180 bp fragment from the SpecR cassette. Order: Positive control (pYES1 new),
728 mutant (CH-2Δwzy), and negative control (distilled water); Lanes 7-9: wzy F and wzy
729 R, which amplify an 886 bp fragment from the wzy gene. Order: Wild-type(CH-2),
730 mutant (CH-2Δ*wzy*), and negative control (distilled water); Lanes 10-11: LSR F and
731 LSR R, which amplify a 1199 bp fragment from the SpecR cassette, indicating that it
732 was inserted in the correct position in the *R. anatipestifer* CH-2 genome. Order:
733 Mutant (CH-2Δ*wzy*), Negative control (distilled water).
734

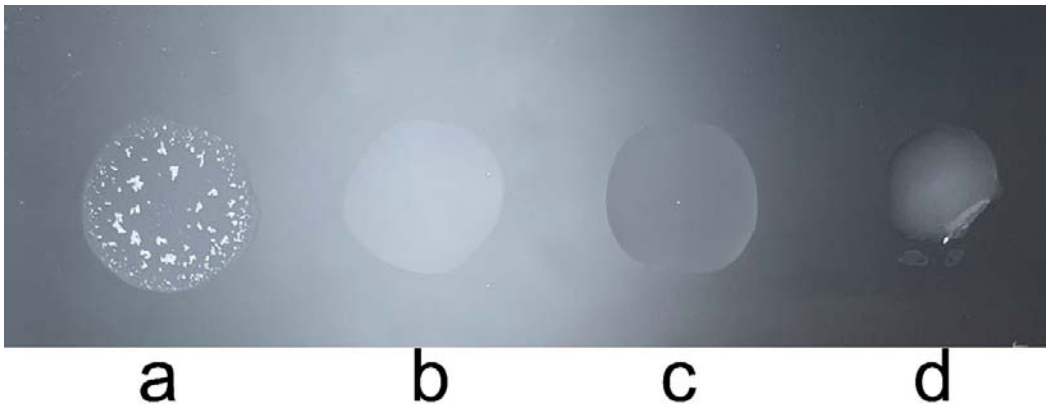

Figure 12. Agglutination test of *R. anatipestifer* CH-2Δ*wzy*. a) Wild-type(CH-2) suspension mixed with antisera of serotype 2; b) mutant(CH-2Δ*wzy*) suspension mixed with antisera of serotype 2; c) distilled water mixed with antisera of serotype 2; and d) mutant(CH-2Δ*wzy*) suspension mixed with distilled water.

Table legends

Table 1. Information of lipopolysaccharide biosynthetic gene cluster of *R. anatipestifer* predicted by antiSMASH.

Table 2. Oligonucleotide primers used in this study

Table 3. Functional prediction of the gene in the O-antigen gene cluster of *R. anatipestifer* (CH-2, serotype 2)

750

751 # Table

752 **Table 1.** Information of lipopolysaccharide biosynthetic gene cluster of *R. anatipestifer* predicted by antiSMASH.

Serotype	Representative strain	Accession No. of Sequence	Start of Cluster	End of Cluster	Most similar known cluster	MIBiG BGC ID
1	ATCC 11845	CP003388	949593	981535	Lipopolysaccharide biosynthetic gene cluster (13% of genes show similarity); O-antigen biosynthesis gene cluster (10% of genes show similarity)	BGC0000775_c1; BGC0000782_c1
2	RA-CH-2	CP004020	911907	941443	Lipopolysaccharide biosynthetic gene cluster (13% of genes show similarity); O-antigen biosynthesis gene cluster (10% of genes show similarity)	BGC0000775_c1; BGC0000782_c1
10	RCAD0146	VLIM00000004	135675	159655	Lipopolysaccharide biosynthetic gene cluster (13% of genes show similarity); O-antigen biosynthesis gene cluster (10% of genes show similarity)	BGC0000775_c1; BGC0000782_c1
11	RCAD0147	LUDN01000002	137494	166627	Lipopolysaccharide biosynthetic gene cluster (13% of genes show similarity); O-antigen biosynthesis gene cluster (10% of genes show similarity)	BGC0000775_c1; BGC0000782_c1

753

754 **Table 2.** Oligonucleotide primers used in this study

Name of primer	Targeted gene; Description	Product Length (bp)		Sequence
Primer_1	ATCC 11845 (RA0C_RS04720); Identification of serotype 1	269	F	CTTGGAGTGCAGAGTCCGAA
			R	AACTCCCATTTCCTCAGCGA
Primer_2	RA-CH-2 (G148_RS04350); Identification of serotype 2	671	F	GCACCTCTTGTTGCCGATTT
			R	ACTGCCTCCTGCCACTTATC
Primer_11	RCAD0147 (AWM66_RS03025); Identification of serotype 11	510	F	GGGATGCGATTAGTGGGGAG
			R	CACATGCGTAGACCACCCTT
Primer_RA	ATCC (RA0C_RS01755); Identification of *R. anatipestifer*	1112	F	GCAGAGGGACAAGCTCCTTT
			R	TGTGCCAACCAATATTGAGCC
wzy-Left	RA-CH-2 (G148_RS04360); Amplification of the *wzy* upstream fragment	609	F	AAGAACATTACCCATATCCTATCGTTTCGACGGTA
			R	TTCTGTCCTGGCTGGTTTTACGAATATTTGTAAGATA
wzy-Right	RA-CH-2 (G148_RS04370); Amplification of the *wzy* downstream fragment	602	F	CCAAGGTAGTCGGCAAATAATTTTATGAAAAAAGTAC
			R	TACATGAGAAACCACAAAAGCCTCTTTGGGAATA
wzy	RA-CH-2 (G148_RS04365); Amplification of the wzy	886	F	TCCAATGGGTTTACTTTCTTGTAACTTTGTCT
			R	CGTAATGGTTGGTTGAGATTCATTGGAG
LSR	G148_RS04360+spec; Identification of transconjugants	1199	F	AGGTAGATAGGGCAAGTATGGCTTTTTCG
			R	ACCGTAACCAGCAAATCAATATCACTGTG
16S rRNA	16S rRNA; Identification of species	960	F	CTTCGGATACTTGAGAGCG
			R	GCAGCACCTTGAAAATTGT
Spec	*spec;* Amplification of the *spec*	1145	F	TCTTACAAATATTCGTAAAACCAGCCAGGACAGAAAT
			R	ACTTTTTTCATAAAATTATTTGCCGACTACCTTGGTG

755

756 **Table 3** Functional prediction of the gene in the O-antigen gene cluster of *R. anatipestifer* (CH-2, serotype 2)

Accession No. of gene	Gene name	Conserved Domains (CDD) Annotation; (E-value)	Similar protein; (GenBank accession No.)	Identities / Positives / Coverage (%)
G148_RS04320	-	COG1086; (0.0)	Capsular polysaccharide biosynthesis protein CapD; (AAS60264.1)	38.37/57.84/75.82
G148_RS04325	*wza*	COG1596; (2.08e-20)	Capsular polysaccharide export protein; (AFH02820.1)	28.38/48.65/49.08
G148_RS04330	*wzc*	TIGR01005; (4.07e-47)	Tyrosine protein kinase; (AIG56889.1)	22.73/43.18/85.57
G148_RS04335	-	cd05256; (3.55e-158)	GlcNAc-4-epimerase; (AAZ85711.1)	56.57/71.87/99.38
G148_RS04340	-	cd16377; (6.83e-45)	Four helix bundle protein; (WP_004918279.1)	100.00/100.00/100
G148_RS04345	-	PRK15182; (0.0)	UDP-GalNAc dehydrogenase; (AAS60268.1)	50.82/68.62/96.24
G148_RS04350	*wzx*	cd13127; (2.33e-90)	O unit flippase Wzx; (ABG81799.1)	33.01/53.11/85.95
G148_RS04355		pfam00535; (1.04e-29)	Glycosyltransferase family 2 protein; (WP_002998031.1)	52.63/72.63/99.30
G148_RS04360	-	TIGR03108; (2.18e-145)	Asparagine synthetase ; (WP_002998029.1)	68.77/85.22/99.50
G148_RS04365	*wzy*	pfam14897; (0.002)	O-antigen polymerase Wzy; (ACD37078.1)	23.41/45.55/86.40
G148_RS04370		cd03807; (1.50e-46)	Glycosyltransferase; (OJX49487.1)	52.22/71.39/99.72
G148_RS04375		cd03798; (1.06e-32)	Glycosyltransferase; (AGC40177.1)	100.00/100.00/100
G148_RS04380	-	TIGR03108; (5.20e-154)	Putative asparagine synthase; (AAO39701.1)	34.37/54.80/96.50
G148_RS04385		cd03808; (2.57e-119)	Glycosyl transferase family 1; (AAS60267.1)	100.00/100.00/100
G148_RS04390	-	pfam14897; (0.001)	Hypothetical protein; (WP_004918298.1)	100.00/100.00/100
G148_RS04395		pfam02397; (3.63e-91)	UDP-galactose phosphate transferase; (ABK81659.1)	58.00/75.50/99.01
G148_RS04400	-	TIGR03570; (4.94e-72)	Acetyltransferase; (ABK81660.1)	33.84/55.56/92.50
G148_RS04405	-	TIGR04181; (6.11e-163)	Aminotransferase; (ABK81658.1)	51.60/71.12/96.29
G148_RS04410		pfam02397; (1.10e-44)	Sugar transferase; (WP_004918306.1)	100.00/100.00/100

G148_RS04415	*rmlC*	pfam00908; (9.91e-105)	dTDP-6-deoxy-D-glucose-3,5 epimerase ; (ACA24909.1)	56.57/70.29/96.13
G148_RS04420	*rmlB*	COG1088; (0.0)	dTDP-Glc 4,6-dehydratase; (AGO01092.1)	56.74/72.47/94.74
G148_RS04425	*rmlA*	TIGR01207; (0.0)	glucose-1-phosphate thymidylyltransferase 1; (AIG62809.1)	69.82/82.46/99.65

757

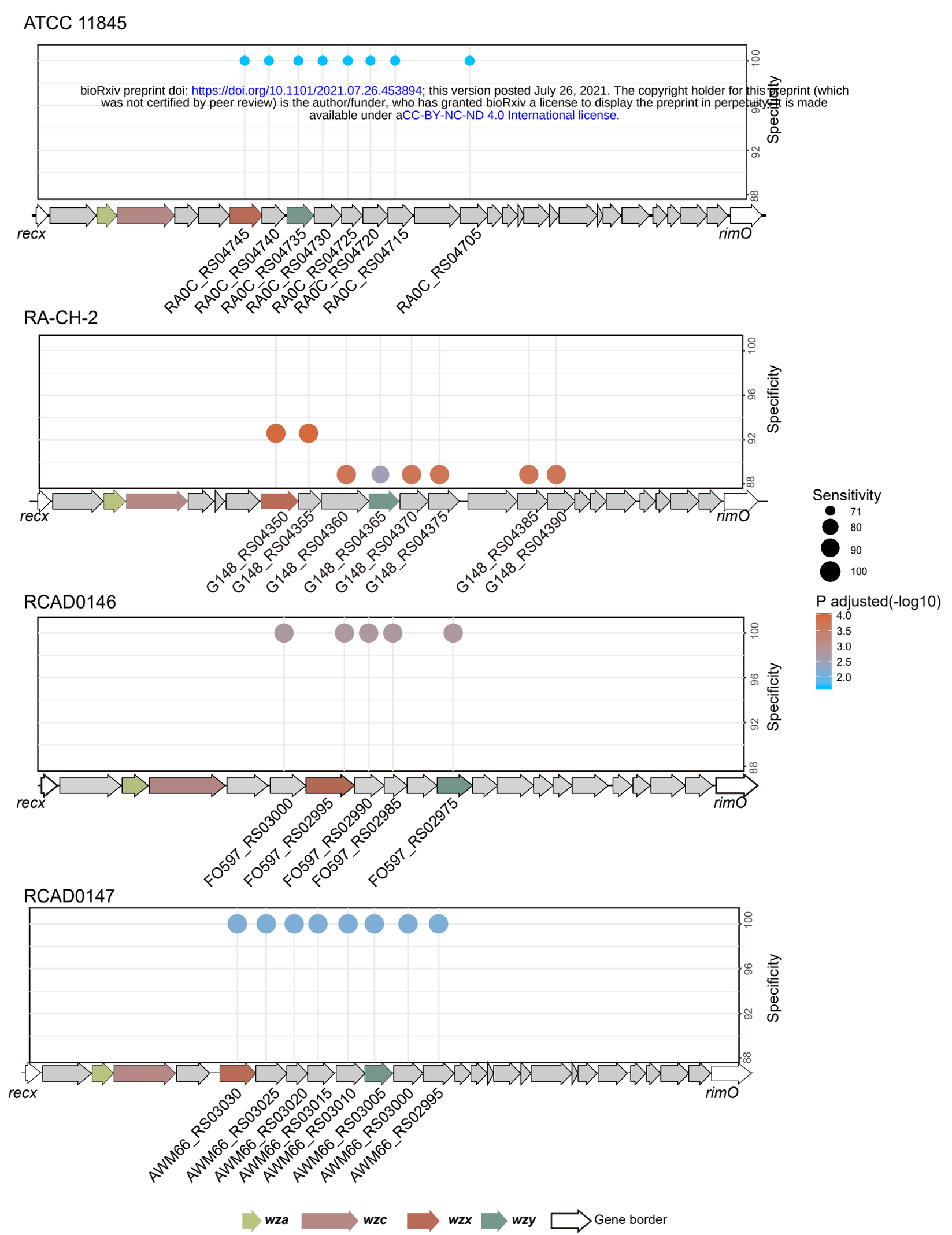

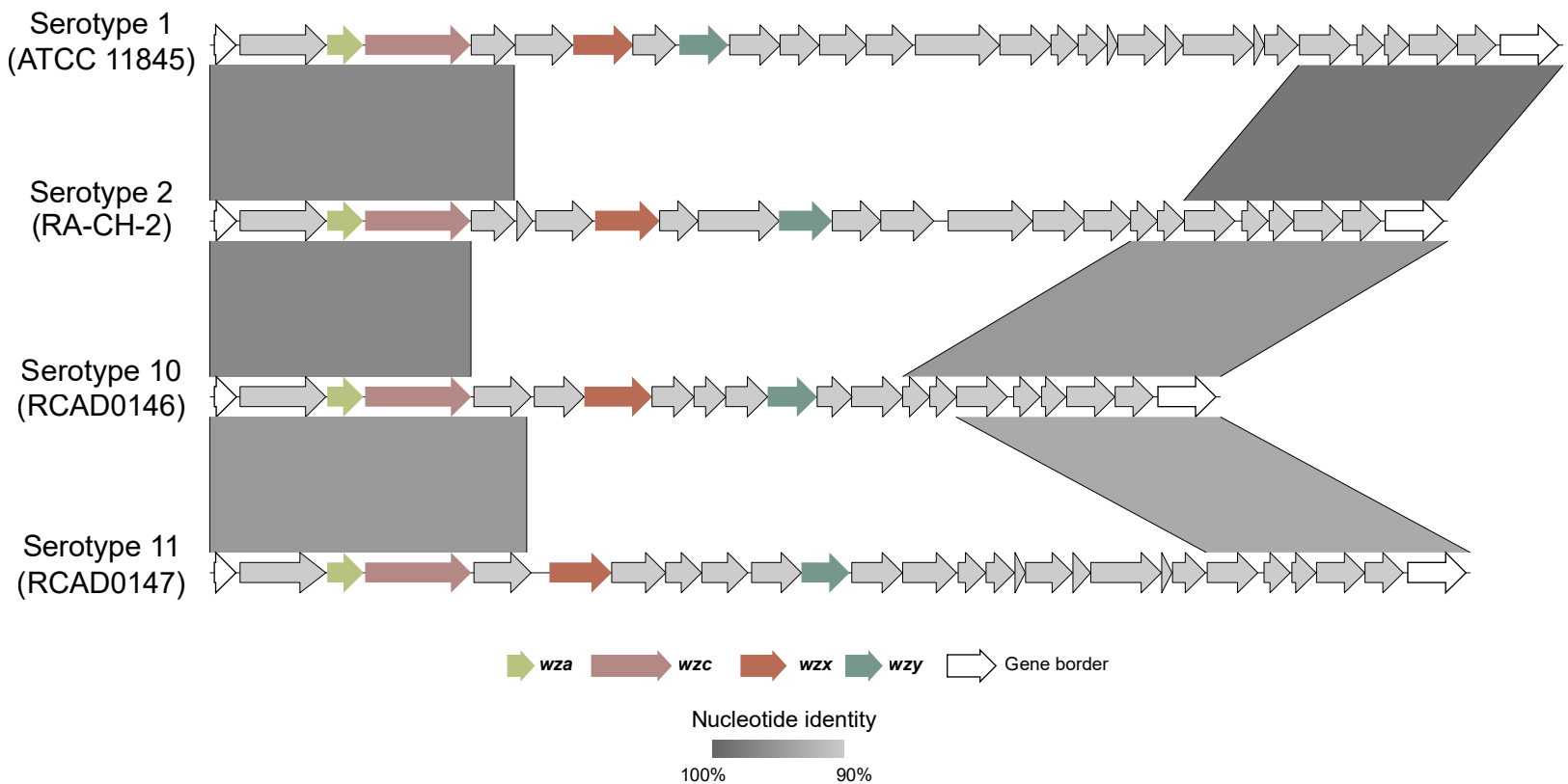
Serotype 1
(ATCC 11845)
Serotype 2
(RA-CH-2)
Serotype 10
(RCAD0146)
Serotype 11
(RCAD0147)
wza
wzc
wzx
wzy
Gene border
Nucleotide identity
100%
90%

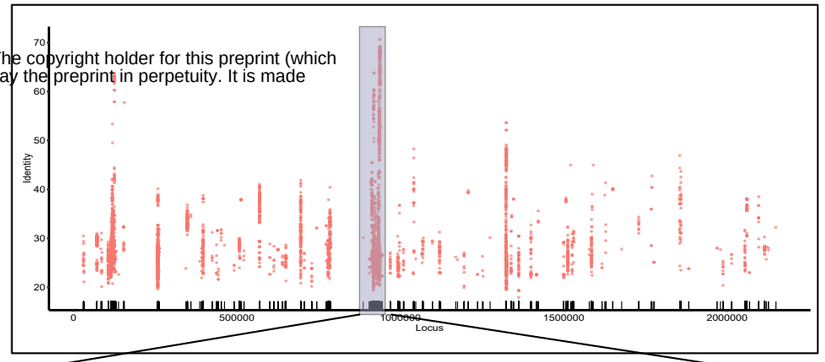

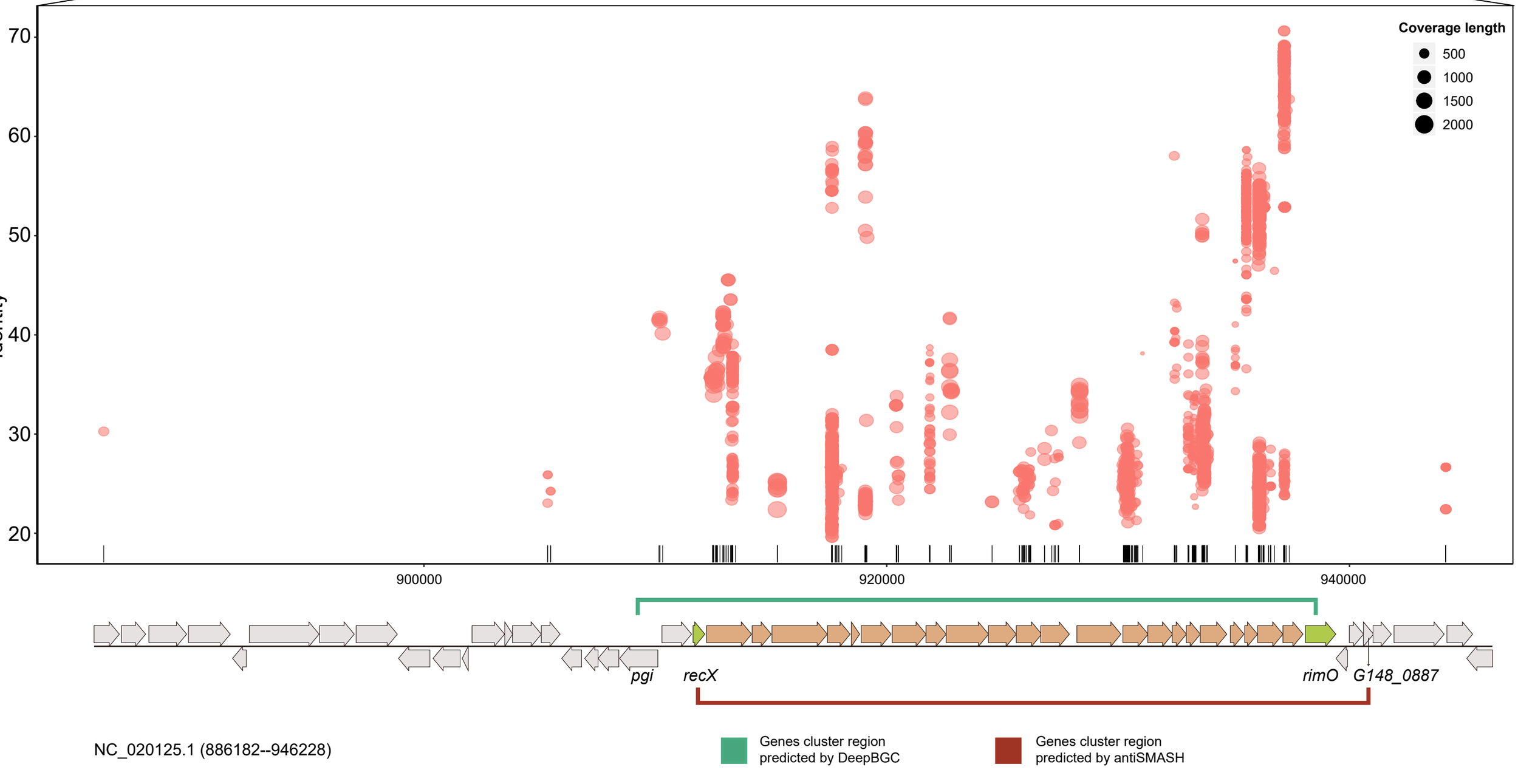

a

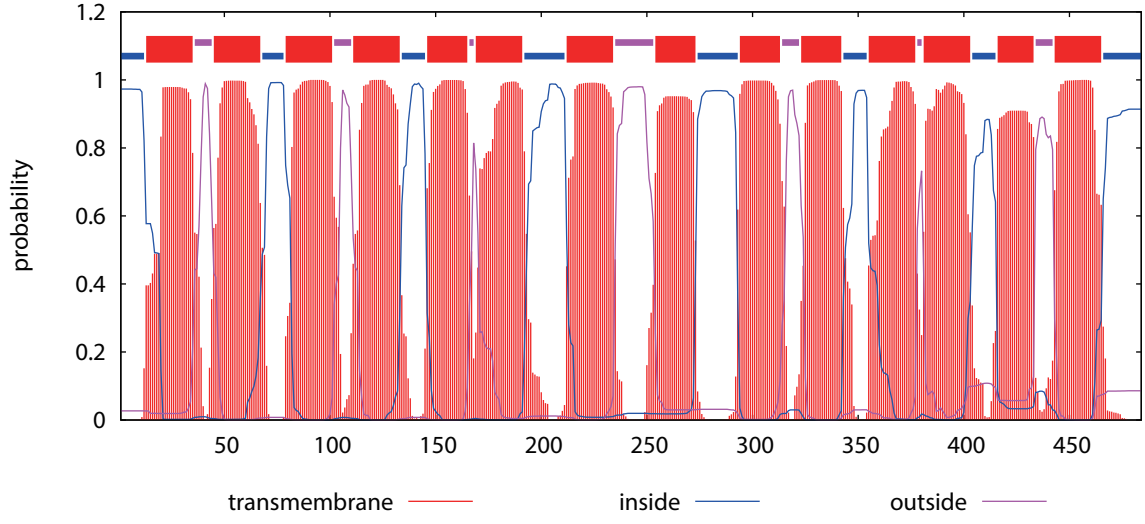
probability
1.2
1
0.8
0.6
0.4
0.2
0
50
100
150
200
250
300
350
400
450
transmembrane
inside
outside

b

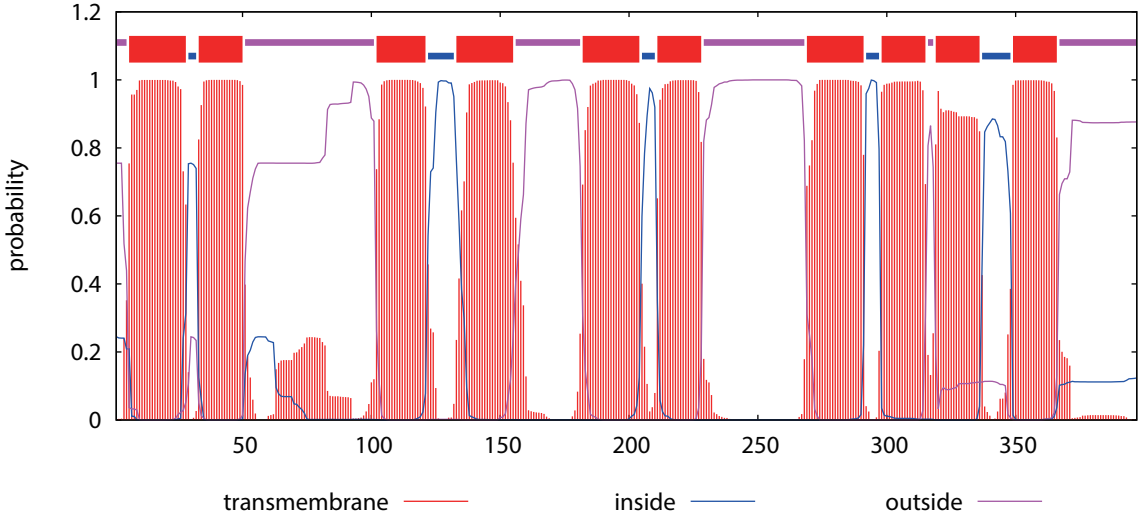
probability
1.2
1
0.8
0.6
0.4
0.2
0
50
100
150
200
250
300
350
transmembrane
inside
outside

Serotype_1

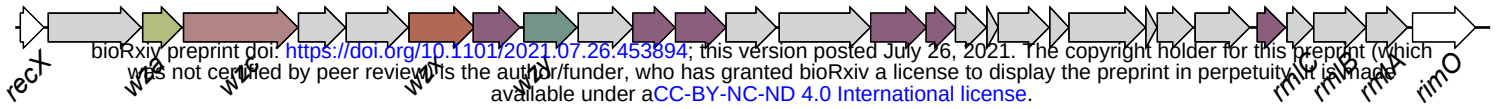

Serotype_2

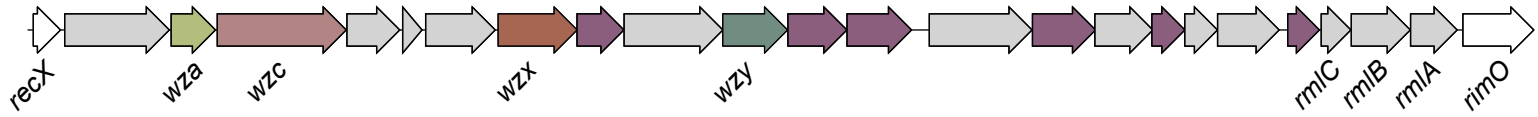

Serotype_3

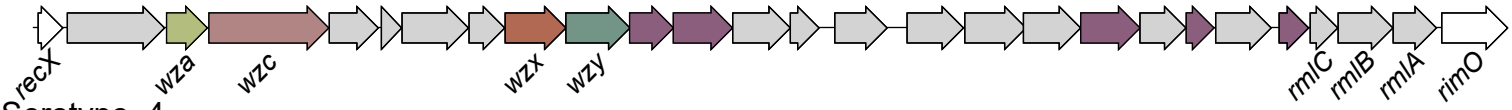

Serotype_4

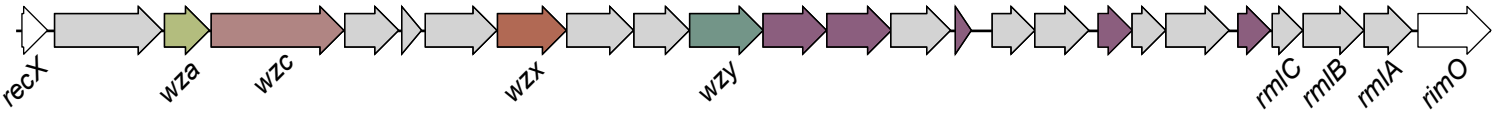

Serotype_5

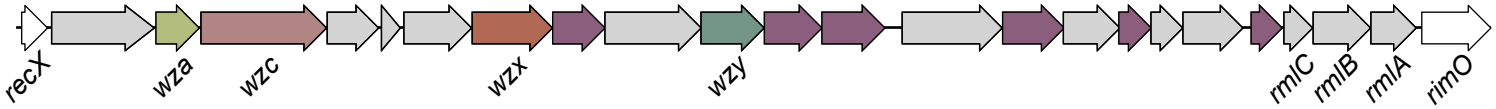

Serotype_6

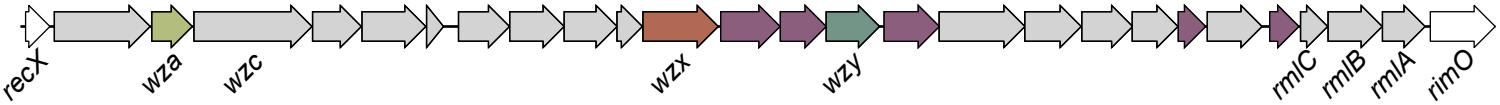

Serotype_7

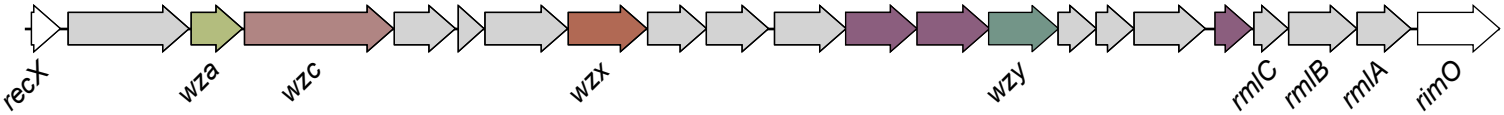

Serotype_8

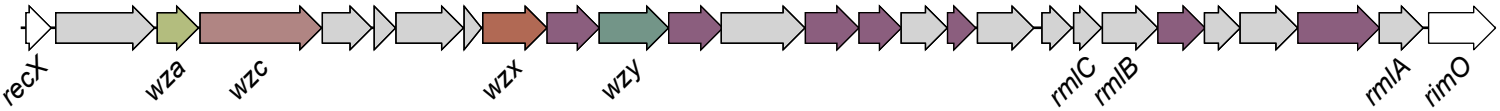

Serotype_10

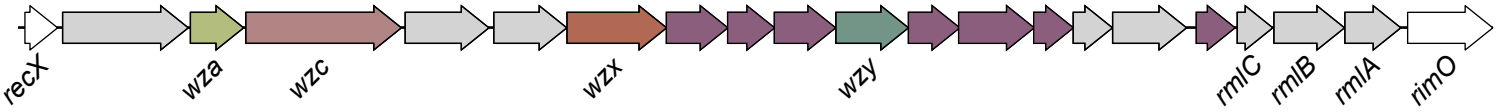

Serotype_11

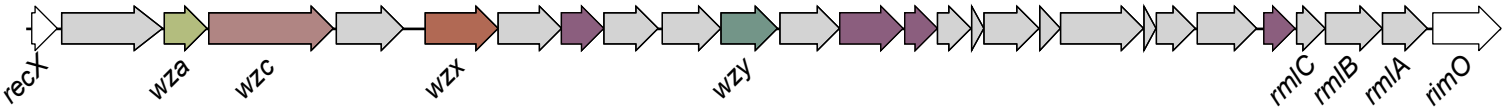

Serotype_12

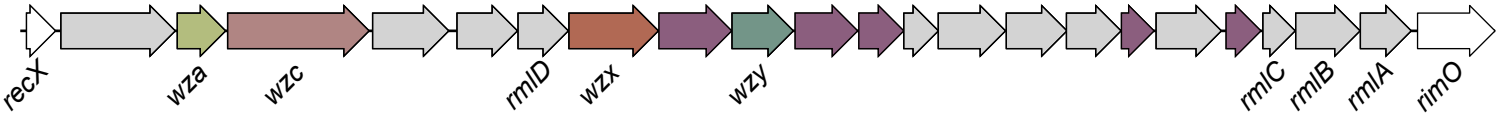

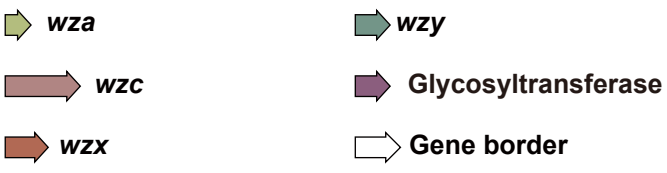

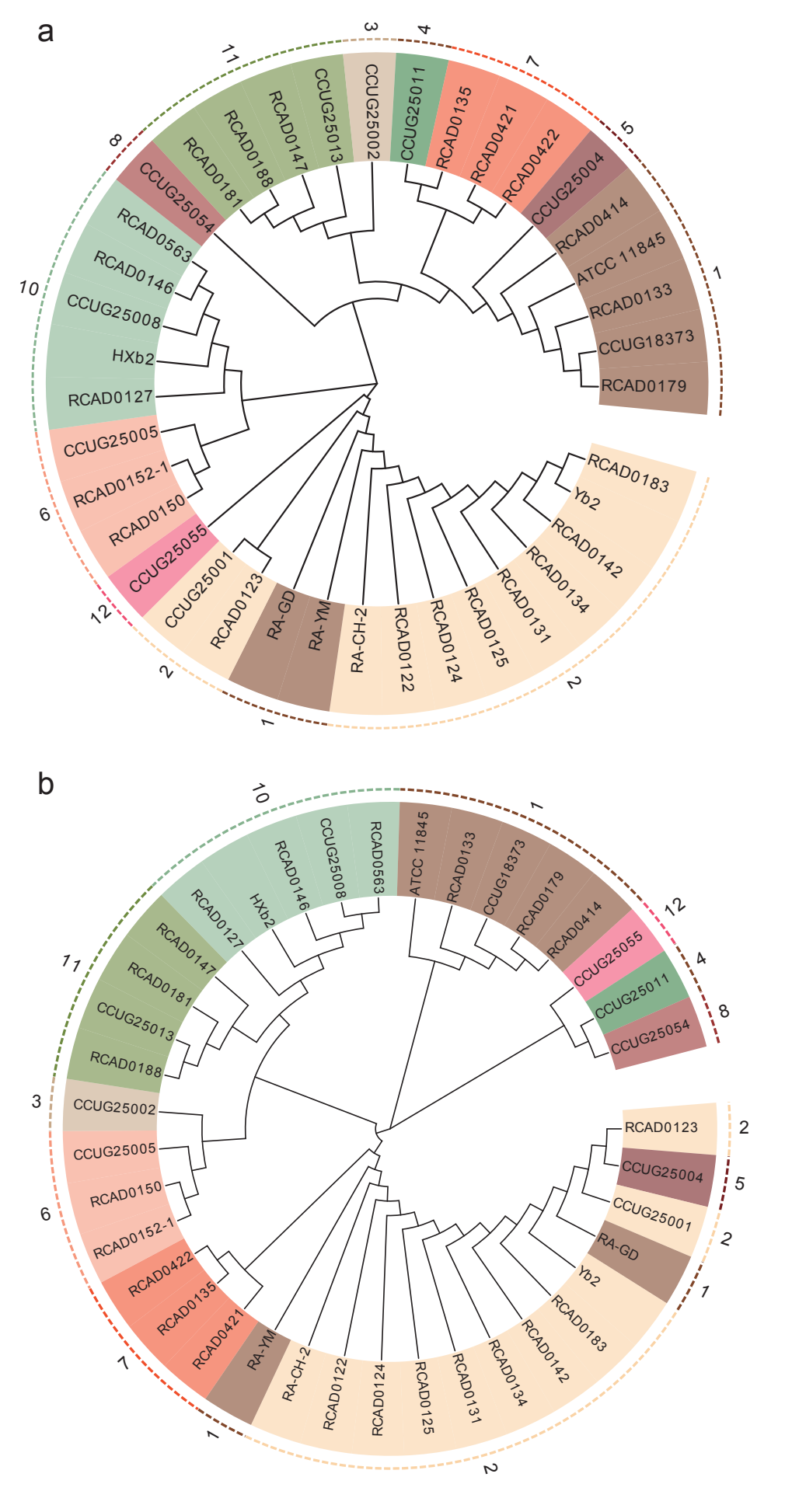
a
CCUG25002
CCUG25011
RCAD0135
RCAD0421
RCAD0422
CCUG25004
RCAD0414
ATCC 11845
RCAD0133
CCUG18373
RCAD0179
RCAD0183
Yb2
RCAD0142
RCAD0134
RCAD0131
RCAD0125
RCAD0124
RCAD0122
RA-CH-2
RA-YM
RA-GD
RCAD0123
CCUG25001
CCUG25055
RCAD0150
RCAD0152-1
CCUG25005
RCAD0127
HXb2
CCUG25008
RCAD0146
RCAD0563
CCUG25054
RCAD0181
RCAD0188
CCUG25013
RCAD0147
b
RCAD0563
CCUG25008
RCAD0146
HXb2
RCAD0127
RCAD0147
RCAD0181
CCUG25013
RCAD0188
CCUG25002
CCUG25005
RCAD0150
RCAD0152-1
RCAD0422
RCAD0135
RCAD0421
RA-YM
RA-CH-2
RCAD0122
RCAD0124
RCAD0125
RCAD0131
RCAD0134
RCAD0142
RCAD0183
Yb2
RA-GD
CCUG25001
CCUG25004
RCAD0123
CCUG25054
CCUG25011
CCUG25055
RCAD0414
RCAD0179
CCUG18373
RCAD0133
ATCC 11845

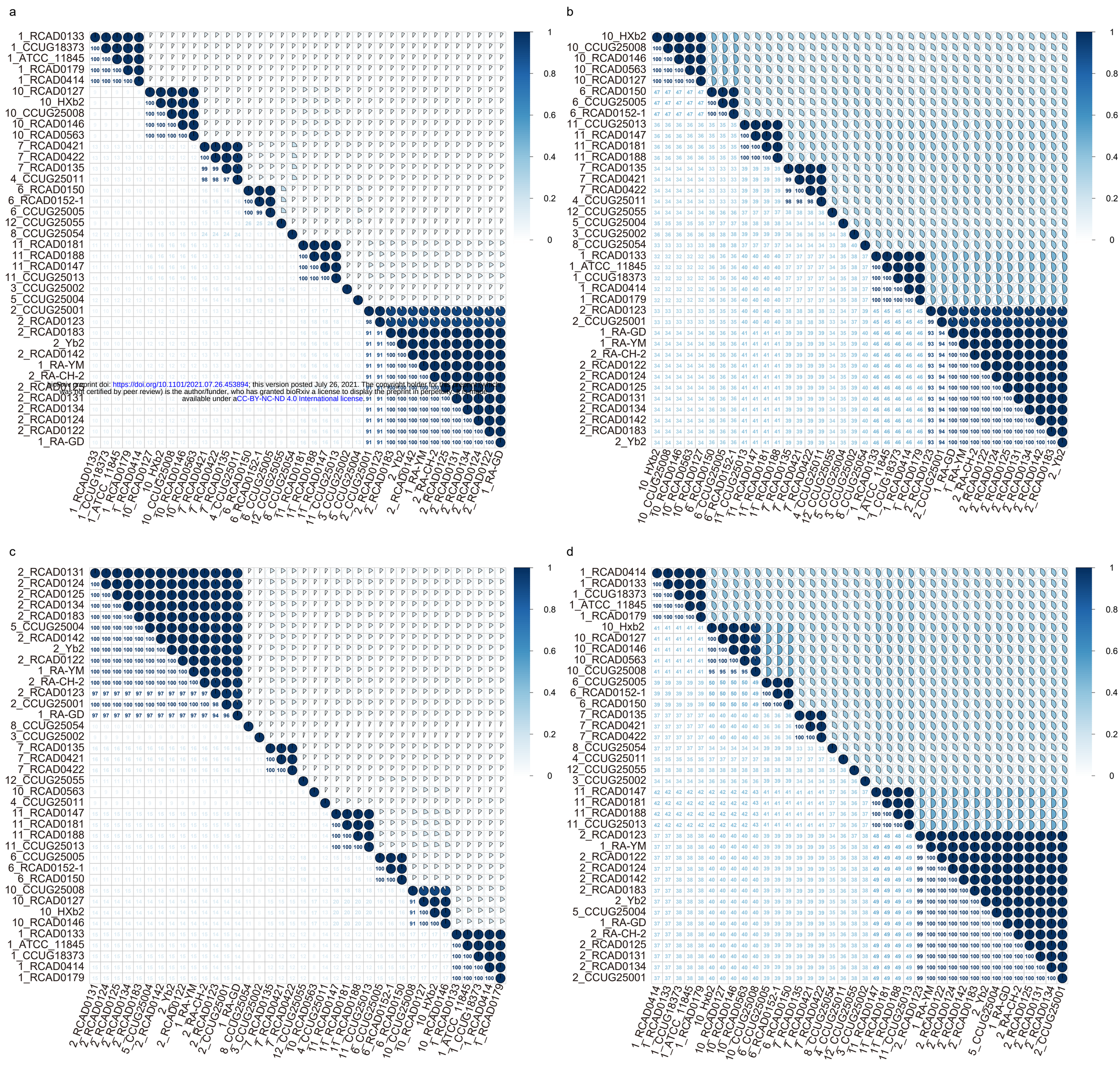

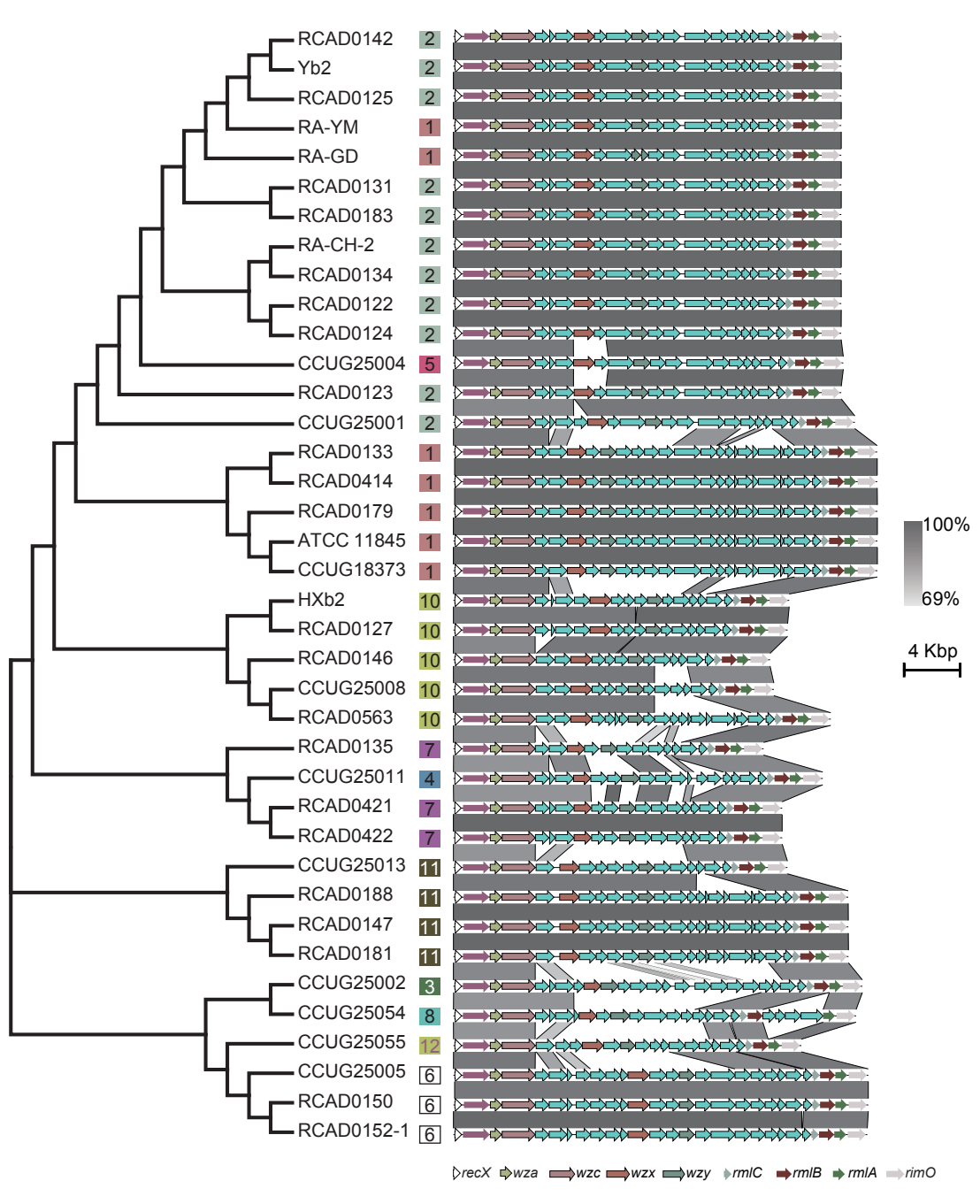
RCAD0142 2
Yb2 2
RCAD0125 2
RA-YM 1
RA-GD 1
RCAD0131 2
RCAD0183 2
RA-CH-2 2
RCAD0134 2
RCAD0122 2
RCAD0124 2
CCUG25004 5
RCAD0123 2
CCUG25001 2
RCAD0133 1
RCAD0414 1
RCAD0179 1
ATCC 11845 1
CCUG18373 1
HXb2 10
RCAD0127 10
RCAD0146 10
CCUG25008 10
RCAD0563 10
RCAD0135 7
CCUG25011 4
RCAD0421 7
RCAD0422 7
CCUG25013 11
RCAD0188 11
RCAD0147 11
RCAD0181 11
CCUG25002 3
CCUG25054 8
CCUG25055 12
CCUG25005 6
RCAD0150 6
RCAD0152-1 6
100%
69%
4 Kbp
recX wza wzc wzx wzy rmlC rmlB rmlA rimO

a

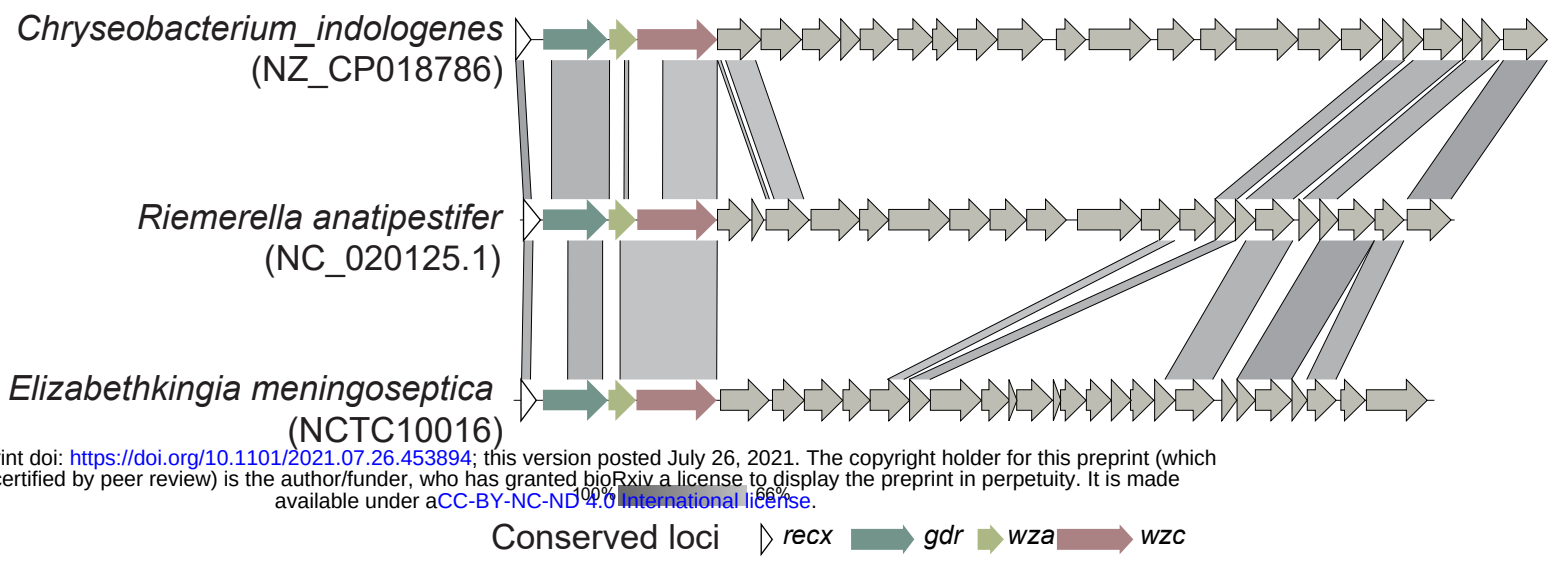

b

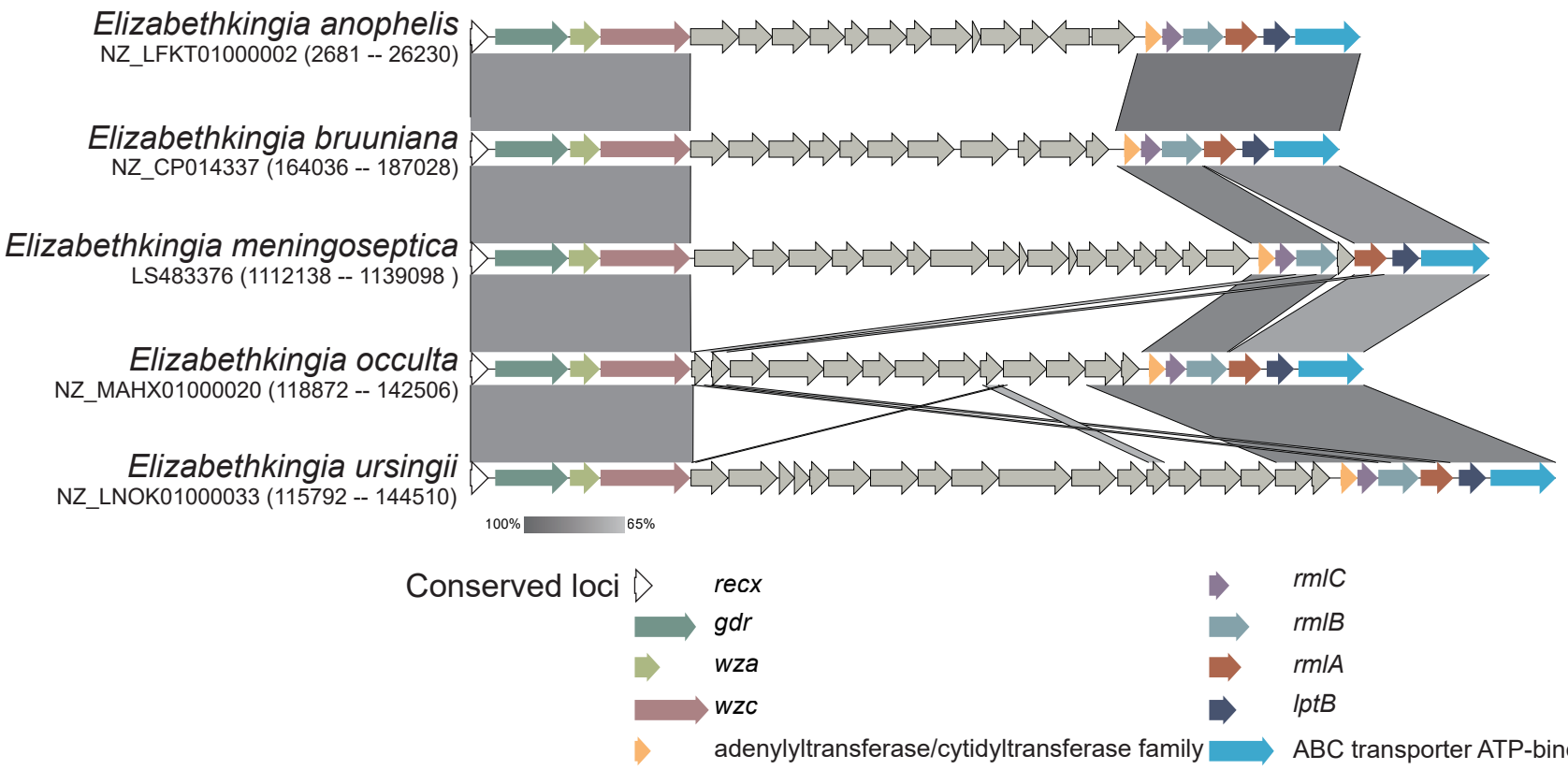

c

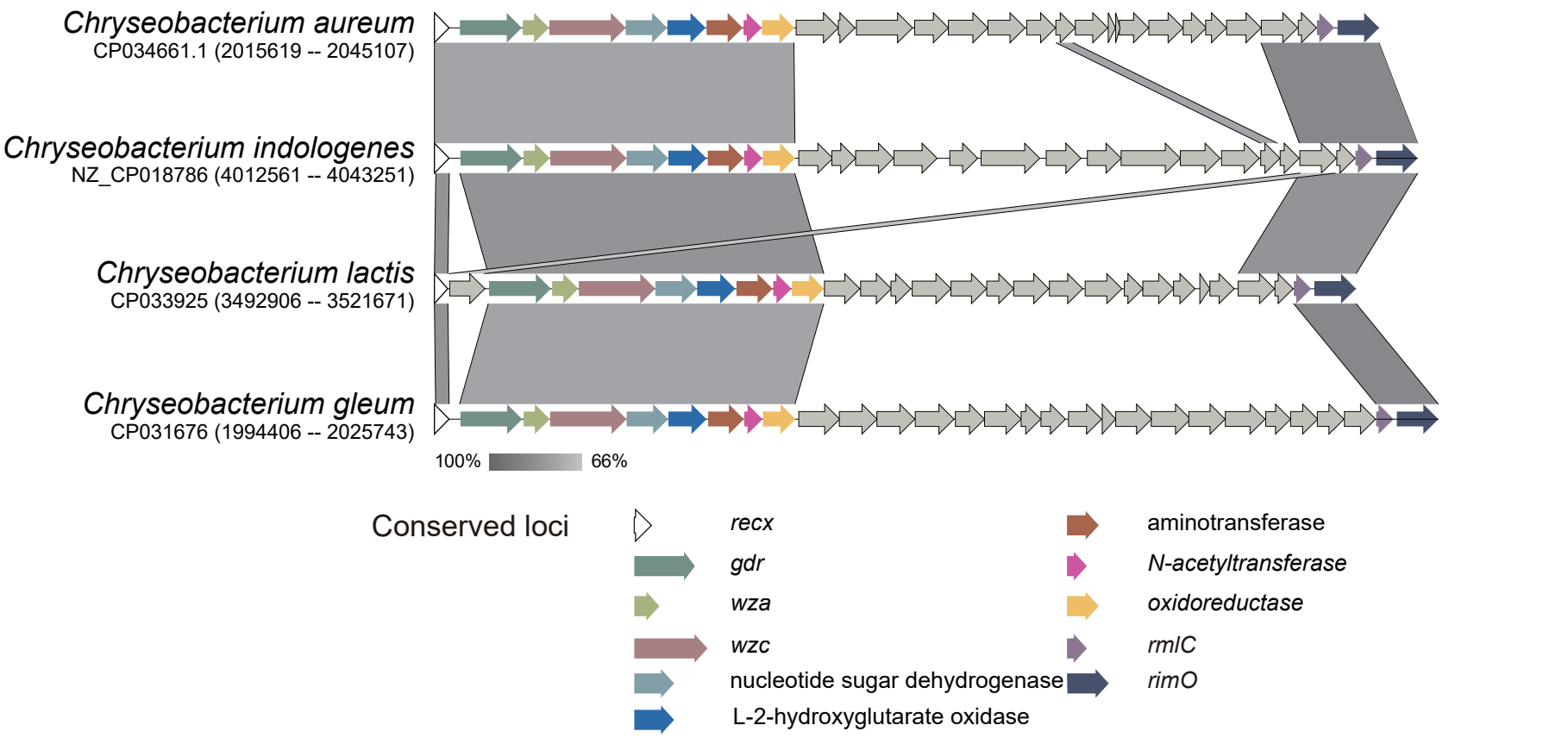

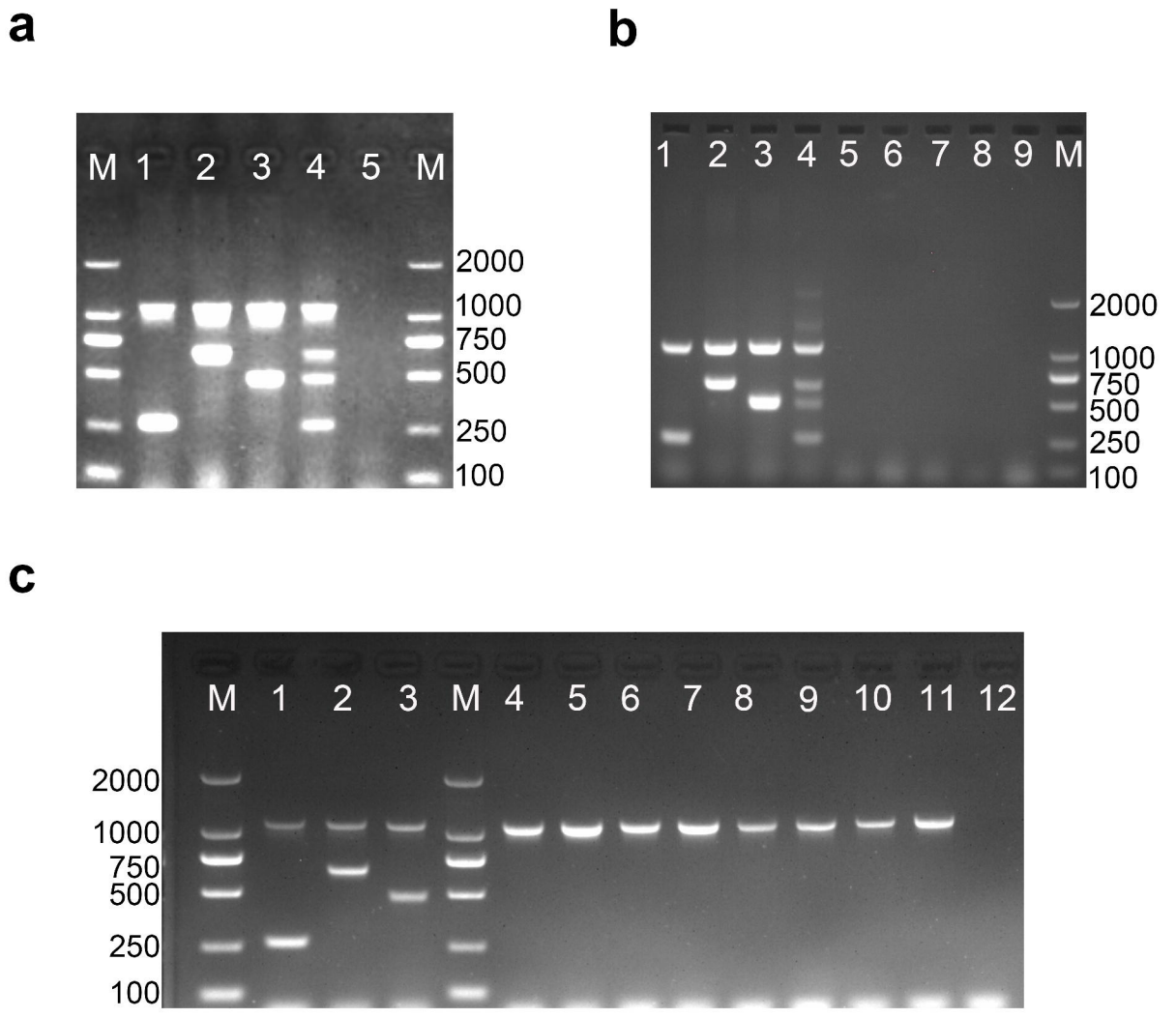
a
M 1 2 3 4 5 M
2000
1000
750
500
250
100
b
1 2 3 4 5 6 7 8 9 M
2000
1000
750
500
250
100
c
M 1 2 3 M 4 5 6 7 8 9 10 11 12
2000
1000
750
500
250
100

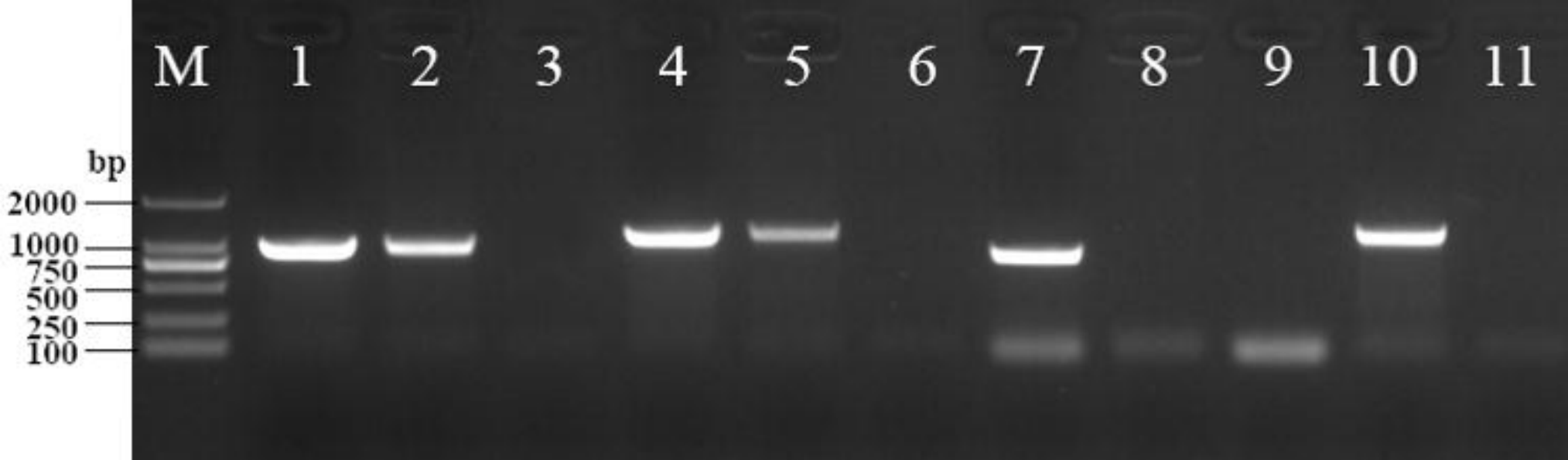
M
1
2
3
4
5
6
7
8
9
10
11
bp
2000
1000
750
500
250
100

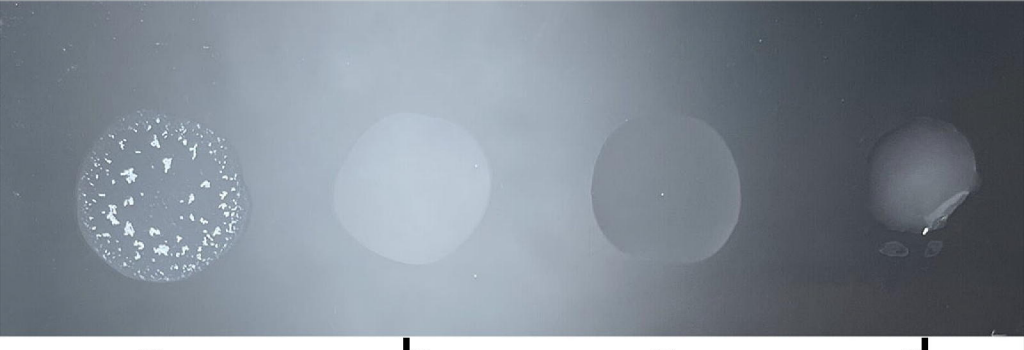
a
b
c
d